

Communication-efficient Vertical Federated Learning via Compressed Error Feedback

Pedro Valdeira^{*†}
CMU & IST

João Xavier[†]
IST

Cláudia Soares[‡]
NOVA

Yuejie Chi^{*}
CMU

June 2024; Revised February 11, 2025

Abstract

Communication overhead is a known bottleneck in federated learning (FL). To address this, lossy compression is commonly used on the information communicated between the server and clients during training. In horizontal FL, where each client holds a subset of the samples, such communication-compressed training methods have recently seen significant progress. However, in their vertical FL counterparts, where each client holds a subset of the features, our understanding remains limited. To address this, we propose an error feedback compressed vertical federated learning (**EF-VFL**) method to train split neural networks. In contrast to previous communication-compressed methods for vertical FL, **EF-VFL** does not require a vanishing compression error for the gradient norm to converge to zero for smooth nonconvex problems. By leveraging error feedback, our method can achieve a $\mathcal{O}(1/T)$ convergence rate for a sufficiently large batch size, improving over the state-of-the-art $\mathcal{O}(1/\sqrt{T})$ rate under $\mathcal{O}(1/\sqrt{T})$ compression error, and matching the rate of uncompressed methods. Further, when the objective function satisfies the Polyak-Łojasiewicz inequality, our method converges linearly. In addition to improving convergence, our method also supports the use of private labels. Numerical experiments show that **EF-VFL** significantly improves over the prior art, confirming our theoretical results. The code for this work can be found at <https://github.com/Valdeira/EF-VFL>.

1 Introduction

Federated learning (FL) is a machine learning paradigm where a set of clients holding local datasets collaborate to train a model without exposing their local data (McMahan et al., 2017; Zhang et al., 2021; Sery et al., 2021). FL can be divided into two categories, based on how the data is partitioned across the clients: *horizontal* FL, where each client holds a different set of samples but all clients share the same features, and *vertical* FL, where each client holds a different subset of features but all clients share the same samples. Note that we cannot gather and redistribute the data because it must remain at the clients. Thus, we do not choose under which category a given task falls. Rather, the category is a consequence of how the data arises.

In this work, we focus on vertical FL (VFL) (Liu et al., 2024). In VFL, a global dataset $\mathcal{D} = \{\xi_n\}_{n=1}^N$ with N samples is partitioned by features across a set of clients $[K] := \{1, \dots, K\}$. Each sample has K disjoint blocks of features $\xi_n = (\xi_{n1}, \dots, \xi_{nK})$ and the local dataset of each client $k \in [K]$ is $\mathcal{D}_k = \{\xi_{nk}\}_{n=1}^N$, where $\mathcal{D} = \bigcup_k \mathcal{D}_k$. Since different datasets \mathcal{D}_k have different features, VFL suits collaborations of clients with complementary types of information, who tend to have fewer competing interests. This can lead to a greater incentive to collaborate, compared to horizontal FL. A common application of VFL is in settings where multiple entities own distinct features concerning a shared set of users and seek to collaboratively train a predictor; for example, WeBank partners with other companies to jointly build a risk model from data regarding shared customers (Cheng et al., 2020).

^{*}Department of Electrical and Computer Engineering, Carnegie Mellon University; email: pvaldeira@cmu.edu.

[†]Institute for Systems and Robotics, Instituto Superior Técnico.

[‡]Department of Computer Science, NOVA School of Science and Technology.

⁴A preliminary version of this work was accepted for publication at EUSIPCO 2024 (Valdeira et al., 2024).

To jointly train a model from $\{\mathcal{D}_k\}$ without sharing local data, split neural networks (Ceballos et al., 2020) are often considered. To learn the parameters \mathbf{x} of such models, we aim to solve the following nonconvex optimization problem:

$$\min_{\mathbf{x} \in \mathbb{R}^d} f(\mathbf{x}) := \frac{1}{N} \sum_{n=1}^N \phi_n(\mathbf{x}_0, \mathbf{h}_{1n}(\mathbf{x}_1), \dots, \mathbf{h}_{Kn}(\mathbf{x}_K)), \quad (1)$$

where $\mathbf{x} := (\mathbf{x}_0, \mathbf{x}_1, \dots, \mathbf{x}_K)$. Here, $\mathbf{h}_{kn}(\mathbf{x}_k) := \mathbf{h}_k(\mathbf{x}_k; \boldsymbol{\xi}_{nk})$ is the *representation* of $\boldsymbol{\xi}_{nk}$ extracted by the local model of client $k \in [K]$, which is parameterized by \mathbf{x}_k . This representation is then sent to the server. The server, in turn, uses $\{\mathbf{h}_{kn}(\mathbf{x}_k)\}_{k=1}^K$ as input to ϕ_n , which corresponds to the composition of the loss function and the *fusion* model and is parameterized by \mathbf{x}_0 .¹

Most FL methods, including ours, assume that the server can communicate with all the clients and that the clients do not communicate with each other. These methods typically require many rounds of client-server communications. Such communications can significantly slow down training. In fact, they can become the main bottleneck during training (Dean et al., 2012; Lian et al., 2017). To address this, a plethora of communication-efficient FL methods have been proposed. In particular, a popular technique to mitigate the communication overhead is lossy compression. Compression operators, or simply compressors, are operators that map a given vector into another vector that is easier to communicate (that is, requires fewer bits).

Optimization methods employing communication compression have seen great success (Seide et al., 2014; Alistarh et al., 2017). Most of these works focus on the prevalent horizontal FL setup and thus consider *gradient* compression, as these are the vectors being communicated in the horizontal setting (Alistarh et al., 2018; Stich et al., 2018). Yet, in vertical FL, the clients send *representations* $\{\mathbf{h}_{kn}(\mathbf{x}_k)\}$ instead. In contrast to gradient compression, compressing these intermediate representations leads the compression-induced error to undergo a nonlinear function ϕ_n before impacting gradient-based updates. Thus, compression in VFL is not covered by these works and our understanding of it remains limited. In fact, to the best of our knowledge, Castiglia et al. (2022) is the only work providing convergence guarantees for compressed VFL. Yet, Castiglia et al. (2022) employs a direct compression method, requiring the compression error to go to zero as the number of gradient steps T increases, achieving a $\mathcal{O}(1/\sqrt{T})$ rate when the compression error is $\mathcal{O}(1/\sqrt{T})$. This makes the method in Castiglia et al. (2022) unsuitable for applications with strict per-round communication limitations, such as bandwidth constraints, and leads to the following question:

Can we design a communication-compressed VFL method that preserves the convergence rate of uncompressed methods without decreasing the amount of compression as training progresses?

1.1 Our contributions

In this work, we answer the question above in the affirmative. Our main contributions are as follows.

- We propose error feedback compressed VFL (EF-VFL), which leverages an error feedback technique to improve the stability of communication-compressed training in VFL.
- We show that our method achieves a convergence rate of $\mathcal{O}(1/T)$ for nonconvex objectives under nonvanishing compression error for a sufficiently large batch size, improving over the state-of-the-art $\mathcal{O}(1/\sqrt{T})$ rate under $\mathcal{O}(1/\sqrt{T})$ compression error of Castiglia et al. (2022), and matching the rate of the centralized setting. We further show that, under the Polyak-Łojasiewicz (PL) inequality, our method converges linearly to the solution, in the full-batch case, and, more generally, to a neighborhood of size proportional to the mini-batch variance, thus obtaining the first linearly convergent compressed VFL method. Unlike the method in Castiglia et al. (2022), EF-VFL supports the use of private labels, broadening its applicability.
- We run numerical experiments and observe empirically that our method improves the state-of-the-art, achieving a better communication efficiency than existing methods.

¹The server often aggregates the representations \mathbf{h}_{kn} via some nonparameterized operation (for example, a sum or an average) before inputting them into the server model. We consider this aggregation to be included in ϕ_n .

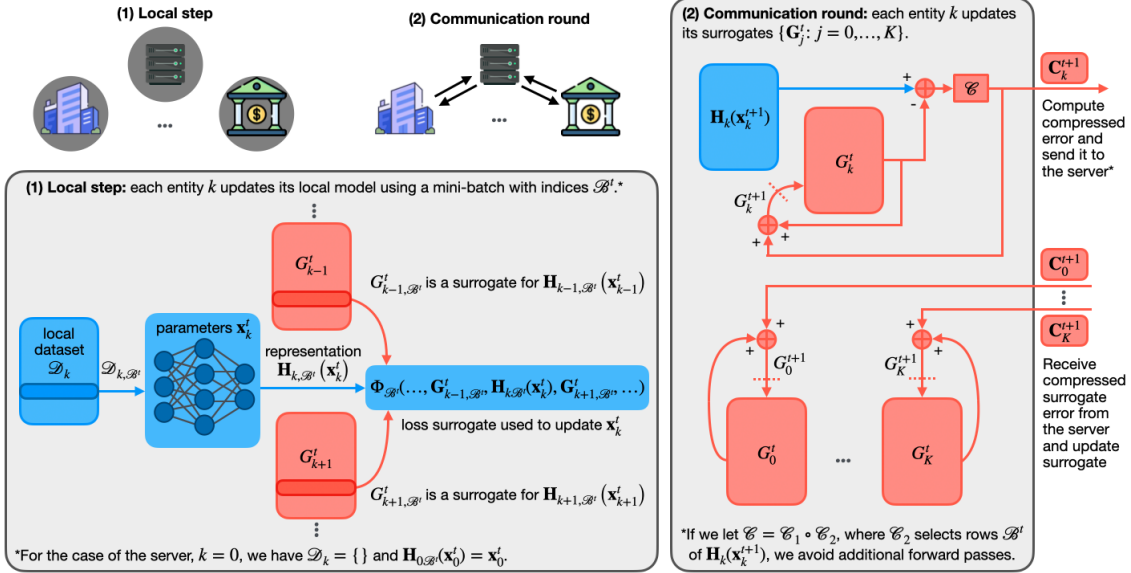


Figure 1: An illustration of an iteration of the EF-VFL algorithm. Step (1) concerns the model update and step (2) concerns the surrogate update.

1.2 Related work

Communication-efficient FL. The aforementioned communication bottleneck in FL (Lian et al., 2017) makes communication-efficient methods a particularly active area of research. FL methods often employ multiple local updates between rounds of communication, use only a subset of the clients at a time (McMahan et al., 2017), or even update the global model asynchronously (Xie et al., 2019). Another line of research considers fully decentralized methods (Lian et al., 2017), dispensing with the server and, instead, exploiting communications between clients. This can alleviate the bandwidth limit ensuing from the centralized role of the server. Another popular technique is lossy compression, which is the focus of this work. In both FL and, more generally, in the broader area of distributed optimization (Chen and Sayed, 2012; Mota et al., 2013), communication-compressed methods have recently received significant attention (Amiri and Gündüz, 2020; Du et al., 2020; Shlezinger et al., 2020; Nassif et al., 2023).

Communication-compressed optimization methods can exploit different families of compressors. A popular choice is the family of *unbiased* compressors (Alistarh et al., 2017), which is appealing in that its properties facilitate the theoretical analysis of the resulting methods. Yet, some widely adopted compressors do not belong to this class, such as top- k sparsification (Alistarh et al., 2018; Stich et al., 2018) and deterministic rounding (Sapio et al., 2021). Thus, the broader family of *contractive* compressors (Beznosikov et al., 2023) has recently attracted a lot of attention. Yet, methods employing them for direct compression are often prone to instability or even divergence (Beznosikov et al., 2023). To address this, error feedback techniques have been proposed; first, as a heuristic (Seide et al., 2014), but, more recently, significant progress has been made on our theoretical understanding of the application of these methods to gradient compression (Stich et al., 2018; Alistarh et al., 2018; Richtárik et al., 2021). In the horizontal setting, some works have combined error feedback compression with the aforementioned communication-efficient techniques, such as communication-compressed fully decentralized methods (Koloskova et al., 2019; Zhao et al., 2022).

Vertical FL. To mitigate the communication bottleneck in VFL, we often employ techniques akin to those used in horizontal FL. In particular, Liu et al. (2022) performed multiple local updates between communication rounds, Chen et al. (2020) updated the local models asynchronously, and Ying et al. (2018) proposed a fully decentralized approach. Recently, Valdeira et al. (2023) proposed a semi-decentralized method leveraging both client-server and client-client communications to avoid the slow convergence of fully-decentralized methods on large and sparse networks while alleviating the server bottleneck.

In this work, we focus on communication-compressed methods tailored to VFL. While, as mentioned above, most work in communication-compressed methods focuses on gradient compression and thus does not apply directly to VFL, recently, a few empirical works on VFL have employed compression. Namely, [Khan et al. \(2022\)](#) compressed the local data before sending it to the server, where the model is trained, and [Li et al. \(2020\)](#) proposed an asynchronous method with bidirectional (sparse) gradient compression. Nevertheless, [Castiglia et al. \(2022\)](#), where direct compression is used, is the only work on compressed VFL with theoretical guarantees. For a more a detailed discussion on VFL, see [Liu et al. \(2024\)](#); [Yang et al. \(2023\)](#).

2 Preliminaries

We now define the class of contractive compressors, which we consider throughout this paper.

Definition 1 (Contractive compressor). *A map $\mathcal{C}: \mathbb{R}^d \mapsto \mathbb{R}^d$ is a contractive compressor if there exists $\alpha \in (0, 1]$ such that,²*

$$\forall \mathbf{v} \in \mathbb{R}^d: \quad \mathbb{E}\|\mathcal{C}(\mathbf{v}) - \mathbf{v}\|^2 \leq (1 - \alpha)\|\mathbf{v}\|^2, \quad (2)$$

where the expectation is taken with respect to the (possible) randomness in \mathcal{C} .

2.1 Error feedback

When transmitting a converging sequence of vectors $\{\mathbf{v}^t\}$, error feedback mechanisms can reduce the compression error compared to direct compression. In communication-compressed optimization, this allows for faster and more stable convergence.

In direct compression, each \mathbf{v}^t is compressed independently, with $\mathcal{C}(\mathbf{v}^t)$ simply replacing \mathbf{v}^t at the receiver. In contrast, in error feedback compression, the receiver employs a surrogate for \mathbf{v}^t that incorporates information from previous steps $i = 0, \dots, t - 1$. This is achieved by resorting to an auxiliary vector that is stored in memory and updated at each step, leveraging *feedback* from the compression of $\{\mathbf{v}^i: i = 0, \dots, t - 1\}$ to refine the surrogate for \mathbf{v}^t .

Earlier communication-compressed optimization methods employing error feedback mechanisms were motivated by sigma-delta modulation ([Inose et al., 1962](#)). In these methods, the auxiliary vector accumulated the compression *error* across steps, adding the accumulated error to the current vector \mathbf{v}^t before compressing and transmitting it ([Seide et al., 2014](#); [Alistarh et al., 2018](#); [Karimireddy et al., 2019](#)).

More recently, a new type of error feedback mechanism has been proposed, where the auxiliary vector \mathbf{s}^t tracks \mathbf{v}^t directly, rather than the accumulated compression error. This mechanism uses the (compressed) difference between \mathbf{v}^{t+1} and \mathbf{s}^t , that is, the *error* of the surrogate, as the feedback. This approach was first introduced in [Mishchenko et al. \(2024\)](#) for unbiased compressors and was later extended to the more general class of contractive compressors in EF21 ([Richtárik et al., 2021](#)). More formally, in EF21, the surrogate \mathbf{s}^t is initialized as $\mathbf{s}^0 = \mathcal{C}(\mathbf{v}^0)$ and updated recursively as:

$$\forall t \geq 0: \quad \mathbf{s}^{t+1} = \mathbf{s}^t + \mathcal{C}(\mathbf{v}^{t+1} - \mathbf{s}^t). \quad (3)$$

Note that, unlike $\mathcal{C}(\mathbf{v}^t)$, \mathbf{s}^t is not necessarily in the range of \mathcal{C} . For example, if \mathcal{C} uses sparsification, then the surrogate at the receiver in direct compression, $\mathcal{C}(\mathbf{v}^t)$, must be sparse, whereas \mathbf{s}^t does not need to be. By continually updating \mathbf{s}^t with the compressed error, we ensure that it tracks \mathbf{v}^t . Moreover, since these updates are compressed, the communication cost remains the same as in direct compression. To maintain consistency, the surrogate \mathbf{s}^t is updated at both the sender (client or server) and the receiver. In this work, we adopt an EF21-based error feedback mechanism and henceforth refer to it simply as error feedback.

²In Definition 1, we use a common, simplified notation, omitting the randomness in $\mathcal{C}: \mathbb{R}^d \times \Omega \rightarrow \mathbb{R}^d$. We assume that the randomness ω in $\mathcal{C}(\mathbf{v}, \omega)$ at different applications of \mathcal{C} is independent.

2.2 Problem setup

Let $\mathbf{h}_{0n}(\mathbf{x}_0) = \mathbf{x}_0$ and $\mathbf{h}_n(\mathbf{x}) = (\mathbf{h}_{0n}(\mathbf{x}_0), \dots, \mathbf{h}_{Kn}(\mathbf{x}_K)) \in \mathbb{R}^E$ where $\mathbf{h}_{kn}(\mathbf{x}_k) \in \mathbb{R}^{E_k}$ and $E = \sum_{k=0}^K E_k$, for all n . Further, let

$$\mathbf{H}_k(\mathbf{x}_k) = \begin{bmatrix} \mathbf{h}_{k1}(\mathbf{x}_k) \\ \vdots \\ \mathbf{h}_{kN}(\mathbf{x}_k) \end{bmatrix} \in \mathbb{R}^{N \times E_k}$$

and

$$\mathbf{H}(\mathbf{x}) := [\mathbf{H}_0(\mathbf{x}_0), \mathbf{H}_1(\mathbf{x}_1), \dots, \mathbf{H}_K(\mathbf{x}_K)] \in \mathbb{R}^{N \times E}.$$

Further, we define $\Phi: \mathbb{R}^{N \times E} \mapsto \mathbb{R}$ as follows:

$$f(\mathbf{x}) = \frac{1}{N} \sum_{n=1}^N \phi_n(\mathbf{h}_n(\mathbf{x})) =: \Phi(\mathbf{H}(\mathbf{x})).$$

Throughout most of the paper, we assume that ϕ_n contains the label of ξ_n and that ϕ_n is known by all the clients and the server. This assumption, known as “relaxed protocol” (Liu et al., 2024), is sometimes made in VFL (Hu et al., 2019; Castiglia et al., 2022, 2023) and has applications, for example, in credit score prediction. We also address the case of private labels, proposing a modified version of our method for that setting in Section 3.1.

We assume that f has an optimal value $f^* := \min_{\mathbf{x}} f(\mathbf{x}) > -\infty$ and make the following assumptions, where ∇ denotes not only the gradient of scalar-valued functions but, more generally, the derivative of a (possibly multidimensional) map.

Assumption 1 (Smoothness). *A function $h: \mathbb{R}^d \mapsto \mathbb{R}$ is L -smooth if there exists a positive constant L such that*

$$\forall \mathbf{x}, \mathbf{y} \in \mathbb{R}^d: \quad \|\nabla h(\mathbf{x}) - \nabla h(\mathbf{y})\| \leq L \|\mathbf{x} - \mathbf{y}\|. \quad (\text{A1})$$

We assume f is L_f -smooth and Φ is L_Φ -smooth and let $L = \max\{L_f, L_\Phi\}$.

Assumption 2 (Bounded derivative). *Map $\mathbf{F}: \mathbb{R}^{p_1} \mapsto \mathbb{R}^{p_2 \times p_3}$ has a bounded derivative if there exists a positive constant H such that*

$$\forall \mathbf{x} \in \mathbb{R}^{p_1}: \quad \|\nabla \mathbf{F}(\mathbf{x})\| \leq H, \quad (\text{A2})$$

where $\|\nabla \mathbf{F}(\mathbf{x})\|$ is the Euclidean norm of the third-order tensor $\nabla \mathbf{F}(\mathbf{x})$. We assume (A2) holds for $\{\mathbf{H}_k\}_{k=0}^K$.

Note that, in Assumption 2, we do *not* assume that our objective function f has a bounded gradient. We only require the local representation-extracting maps $\{\mathbf{H}_k\}$ to have a bounded derivative. The same assumption is also made in Castiglia et al. (2022).

3 Proposed method

To solve Problem (1) with a gradient-based method, we need to perform a forward and a backward pass at each step t to compute the gradient of our objective function. In VFL, a standard uncompressed algorithm employing a single local update per communication round is mathematically equivalent to gradient descent.³ This algorithm, which our method recovers if we set \mathcal{C} to be the identity map, is as follows:

- In the forward pass, each client k computes $\mathbf{H}_k(\mathbf{x}_k^t)$ and sends it to the server, which then computes $f(\mathbf{x}^t) = \Phi(\mathbf{H}(\mathbf{x}^t))$.
- In the backward pass, first, the server backpropagates through Φ , obtaining $\nabla_0 \Phi(\mathbf{x}_0^t, \{\mathbf{H}_k(\mathbf{x}_k^t)\}_{k=1}^K) = \nabla_0 f(\mathbf{x}^t)$ and $\nabla_k \Phi(\{\mathbf{H}_k(\mathbf{x}_k^t)\})$, for all k , where ∇_k denotes the derivative with respect to block k . The former is used to update \mathbf{x}_0^t , while the latter is sent to each client k , which uses this derivative to continue backpropagation over its local model, allowing it to compute $\nabla_k f(\mathbf{x}^t)$.

We repeat these steps until convergence. Let us now cover the general case, where \mathcal{C} may not be the identity map.

³When performing multiple local updates, we lose this mathematical equivalence. In that case, we instead get a parallel (block) coordinate descent method where the simultaneous updates use stale information about the other blocks of variables.

Algorithm 1: EF-VFL

- Input:** initial point \mathbf{x}^0 , stepsize η , and initial surrogates $\{\mathbf{G}_k^0 = \mathcal{C}(\mathbf{H}_k(\mathbf{x}_k^0))\}$.
- 1 **for** $t = 0, \dots, T - 1$ **do**
 - 2 Update $\mathbf{x}_k^{t+1} = \mathbf{x}_k^t - \eta \tilde{\mathbf{g}}_k^t$ in parallel, for $k \in \{0, 1, \dots, K\}$, based on a shared sample $\mathcal{B}^t \subseteq [N]$.
 - 3 Compute and send $\mathbf{C}_k^{t+1} = \mathcal{C}(\mathbf{H}_k(\mathbf{x}_k^{t+1}) - \mathbf{G}_k^t)$ to the server in parallel, for $k \in [K]$.
 - 4 Server broadcasts $\{\mathbf{C}_k^{t+1}\}_{k=0}^K$ to all clients.
 - 5 Update $\mathbf{G}_k^{t+1} = \mathbf{G}_k^t + \mathbf{C}_k^{t+1}$ in parallel, for $k \in \{0, 1, \dots, K\}$.
-

Forward pass. An exact forward pass would require each client k to send $\mathbf{H}_k(\mathbf{x}_k^t)$ to the server, bringing a significant communication overhead. To address this, in our method, the server model does not have as input $\mathbf{H}_k(\mathbf{x}_k^t)$, but rather a surrogate for it, \mathbf{G}_k^t , which is initialized as $\mathbf{G}_k^0 = \mathcal{C}(\mathbf{H}_k(\mathbf{x}_k^0))$ and is updated as follows, as in (3):

$$\forall k \in [K] : \quad \mathbf{G}_k^t := \mathbf{G}_k^{t-1} + \mathbf{C}_k^t, \quad \mathbf{C}_k^t := \mathcal{C}(\mathbf{H}_k(\mathbf{x}_k^t) - \mathbf{G}_k^{t-1}).$$

This requires keeping \mathbf{G}_k^t , of size $N \times E_k$, in memory at client k and at the server. (Note that \mathbf{G}_k^t is often smaller than the local dataset \mathcal{D}_k .) The server thus computes the function $\Phi(\mathbf{x}_0^t, \mathbf{G}_1^t, \dots, \mathbf{G}_K^t)$, which acts as a surrogate for the original objective $f(\mathbf{x}^t) = \Phi(\mathbf{x}_0^t, \mathbf{H}_1(\mathbf{x}_1^t), \dots, \mathbf{H}_K(\mathbf{x}_K^t))$, as illustrated in Figure 1.

Backward pass. The server performs a backward pass over the server model, obtaining $\nabla_0 \Phi(\mathbf{x}_0^t, \{\mathbf{G}_k^t\}_{k=1}^K)$, which it uses as a surrogate for $\nabla_0 \Phi(\mathbf{x}_0^t, \{\mathbf{H}_k(\mathbf{x}_k^t)\}_{k=1}^K) = \nabla_0 f(\mathbf{x}^t)$ to update \mathbf{x}_0^t . Similarly, to update each local model \mathbf{x}_k^t , for $k \in [K]$, we want client k to have a surrogate for

$$\nabla_k f(\mathbf{x}^t) = \sum_{i,j=1}^{N, E_k} [\nabla_k \Phi(\{\mathbf{H}_k(\mathbf{x}_k^t)\}_{k=0}^K)]_{ij} [\nabla \mathbf{H}_k(\mathbf{x}_k^t)]_{ij}.$$

However, while $\nabla \mathbf{H}_k(\mathbf{x}_k^t)$ can be computed at each client k , the $\nabla_k \Phi$ term cannot, as client k does not have access to $\mathbf{H}_\ell(\mathbf{x}_\ell^t)$, for $\ell \neq k$. So, we instead use the following surrogate for $\nabla_k f(\mathbf{x}^t)$:

$$\mathbf{g}_k^t := \sum_{i,j=1}^{N, E_k} [\tilde{\nabla}_k^t \Phi]_{ij} [\nabla \mathbf{H}_k(\mathbf{x}_k^t)]_{ij}, \quad (4)$$

where $\tilde{\nabla}_k^t \Phi := \nabla_k \Phi(\dots, \mathbf{G}_{k-1}^t, \mathbf{H}_k(\mathbf{x}_k^t), \mathbf{G}_{k+1}^t, \dots)$. Since the server does not hold $\mathbf{H}_k(\mathbf{x}_k^t)$, it cannot compute $\tilde{\nabla}_k^t \Phi$. Thus, the server broadcasts $\{\mathbf{C}_k^t\}_{k=0}^K$, so that each client k , which does hold $\mathbf{H}_k(\mathbf{x}_k^t)$, can compute $\{\mathbf{G}_\ell^t\}_{\ell \neq k}$ and use it to perform a forward and a backward pass over the server model locally, obtaining $\tilde{\nabla}_k^t \Phi$. Thus, while the forward pass only requires the error feedback module at each client k to hold the estimate \mathbf{G}_k^t , when we account for the backward pass too, each machine $k \in \{0, 1, \dots, K\}$ must hold $\{\mathbf{G}_\ell^t\}_{\ell=0}^K$. We write our update as:

$$\mathbf{x}^{t+1} = \mathbf{x}^t - \eta \mathbf{g}^t \quad \text{where} \quad \mathbf{g}^t := (\mathbf{g}_0^t, \dots, \mathbf{g}_K^t)$$

and η is the stepsize.

Mini-batch. For the sake of computation efficiency, we further allow for the use of mini-batch approximations of the objective. Without compression, or with direct compression, the use of mini-batches allows client k to send only the entries of $\mathbf{H}_k(\mathbf{x}_k)$ corresponding to mini-batch $\mathcal{B} \subseteq [N]$, of size B , denoted by $\mathbf{H}_{k\mathcal{B}}(\mathbf{x}_k) \in \mathbb{R}^{B \times E_k}$, instead of $\mathbf{H}_k(\mathbf{x}_k) \in \mathbb{R}^{N \times E_k}$. Yet, our method provides all machines with an estimate for all the entries of $\{\mathbf{H}_k(\mathbf{x}_k)\}$ at all times, the error feedback states $\{\mathbf{G}_k\}$. Therefore, our communications, needed to update \mathbf{G}_k , may not depend on N and B at all. This is determined by our choice of \mathcal{C} .

Our mini-batch surrogates depend on the entries of $\mathbf{H}_k(\mathbf{x}_k)$ and \mathbf{G}_k corresponding to \mathcal{B} , $\mathbf{H}_{k\mathcal{B}}(\mathbf{x}_k)$ and $\mathbf{G}_{k\mathcal{B}}$. (Note that $\mathbf{H}_{0\mathcal{B}}(\mathbf{x}_0) = \mathbf{H}_0(\mathbf{x}_0)$ and $\mathbf{G}_{0\mathcal{B}}^t = \mathbf{G}_0^t$.) Thus, we approximate the partial derivative of the

mini-batch function $f_{\mathcal{B}}(\mathbf{x}) = \Phi_{\mathcal{B}}(\{\mathbf{H}_{k\mathcal{B}}(\mathbf{x}_k)\}) = \frac{1}{B} \sum_{n \in \mathcal{B}} \phi_n(\mathbf{h}_n(\mathbf{x}))$ with respect to \mathbf{x}_k by:

$$\tilde{\mathbf{g}}_k^t := \sum_{i \in \mathcal{B}^t} \sum_{j=1}^{E_k} \left[\tilde{\nabla}_k^t \Phi_{\mathcal{B}^t} \right]_{ij} \left[\nabla \mathbf{H}_{k\mathcal{B}^t}(\mathbf{x}_k^t) \right]_{ij},$$

where $\tilde{\nabla}_k^t \Phi_{\mathcal{B}^t} := \nabla_k \Phi_{\mathcal{B}^t}(\dots, \mathbf{G}_{k-1, \mathcal{B}^t}^t, \mathbf{H}_{k\mathcal{B}^t}(\mathbf{x}_k^t), \mathbf{G}_{k+1, \mathcal{B}^t}^t, \dots)$. We write the mini-batch version of the update as:

$$\mathbf{x}^{t+1} = \mathbf{x}^t - \eta \tilde{\mathbf{g}}^t \quad \text{where} \quad \tilde{\mathbf{g}}^t := (\tilde{\mathbf{g}}_0^t, \dots, \tilde{\mathbf{g}}_K^t).$$

We now describe our method, which we summarize in Algorithm 1.

- **Initialization:** We initialize our model parameters as \mathbf{x}^0 . Each machine $k \in \{0, 1, \dots, K\}$ must hold \mathbf{x}_k^0 and our compression estimates $\{\mathbf{G}_k^0 = \mathcal{C}(\mathbf{H}_k(\mathbf{x}_k^0))\}_{k=0}^K$.
- **Model parameters update:** In parallel, all machines $k \in \{0, 1, \dots, K\}$ take a (stochastic) coordinate descent step with respect to their local surrogate objective, updating $\mathbf{x}_k^{t+1} = \mathbf{x}_k^t - \eta \tilde{\mathbf{g}}_k^t$ based on a shared batch \mathcal{B}^t , sampled locally at each client following a shared seed.
- **Compressed communications:** All clients $k \in [K]$ compute \mathbf{C}_k^{t+1} and send it to the server, who broadcasts $\{\mathbf{C}_k^{t+1}\}$.
- **Compression estimates update:** Lastly, all machines $k \in \{0, 1, \dots, K\}$ use the compressed error feedback $\{\mathbf{C}_k^{t+1}\}$ to update their (matching) compression estimates $\{\mathbf{G}_k^t\}$.

Note that, in the absence of compression (that is, if \mathcal{C} is the identity operator), each client k must send \mathbf{C}_k^{t+1} , of size $N \times E_k$, at each iteration. Further, the server must broadcast $\{\mathbf{C}_k^{t+1}\}_{k=0}^K$. Thus, the total communication complexity of EF-VFL in the absence of compression is $\mathcal{O}(N \cdot E \cdot T)$. When compression is used, $N \cdot E$ is replaced by some smaller amount which depends on the compression mechanism. For example, for top- k sparsification (defined in Section 5), the communication complexity is reduced to $\mathcal{O}(k \cdot T)$.

In Algorithm 1, we formulate our method in a general setting which allows for the compression of both $\{\mathbf{H}_k(\mathbf{x}_k)\}_{k=1}^K$ and \mathbf{x}_0 . This setting is covered by our analysis in Section 4. However, in general, the bottleneck lies in the uplink (client-to-server) communications, rather than the server broadcasting (Haddadpour et al., 2021). Therefore, our experiments in Section 5 focus on the compression of $\{\mathbf{H}_k(\mathbf{x}_k)\}_{k=1}^K$, rather than \mathbf{x}_0 .

3.1 Adapting our method for handling private labels

In this section, we propose an adaptation of EF-VFL to allow for private labels. That is, we remove the assumption that all clients hold ϕ_n , which contains the label of ξ_n . Instead, only the server holds the labels. Further, in this adaptation, the parameters of the server model, \mathbf{x}_0 , are not shared with the clients either.

Note that, without holding ϕ_n , the clients cannot perform the entire forward pass locally. Instead, in this setting, the forward and backward pass over ϕ_n take place at the server, while the forward and backward pass over $\mathbf{H}_k(\mathbf{x}_k)$ takes place at client k . More precisely, in the forward pass, each client k sends \mathbf{C}_k to the server, who holds \mathbf{x}_0 and the labels, and can thus compute the loss. Then, for the backward pass, the server backpropagates over its model and sends only the derivative of the loss function with respect to \mathbf{G}_k to each client k . This requires replacing our surrogate of $\nabla_k f(\mathbf{x}^t)$ in (4), which uses the exact local representation $\mathbf{H}_k(\mathbf{x}_k)$ at each client, by one based on our error feedback surrogates:

$$\nabla_k^t := \sum_{i,j=1}^{N, E_k} \left[\nabla_k \Phi(\mathbf{H}_0(\mathbf{x}_0^t), \{\mathbf{G}_j^t\}_{j=1}^K) \right]_{ij} \left[\nabla \mathbf{H}_k(\mathbf{x}_k^t) \right]_{ij}. \quad (5)$$

Note that we do not backpropagate through the error-feedback update.

More generally, we use the following (possibly) mini-batch update vector:

$$\underbrace{\sum_{i \in \mathcal{B}^t} \sum_{j=1}^{E_k} \left[\nabla_k \Phi_{\mathcal{B}^t}(\mathbf{H}_{0\mathcal{B}^t}(\mathbf{x}_0^t), \{\mathbf{G}_{j\mathcal{B}^t}^t\}_{j=1}^K) \right]_{ij} \left[\nabla \mathbf{H}_{k\mathcal{B}^t}(\mathbf{x}_k^t) \right]_{ij}}_{=: \tilde{\nabla}_k^t}$$

Algorithm 2: EF-VFL with private labels

- Input:** initial point \mathbf{x}^0 , stepsize η , and initial surrogates $\{\mathbf{G}_k^0 = \mathcal{C}(\mathbf{H}_k(\mathbf{x}_k^0))\}$.
- 1 **for** $t = 0, \dots, T - 1$ **do**
 - 2 Update $\mathbf{x}_k^{t+1} = \mathbf{x}_k^t - \eta \tilde{\nabla}_k^t$ in parallel, for $k \in \{0, 1, \dots, K\}$, based on a shared sample $\mathcal{B}^t \subseteq [N]$.
 - 3 Compute and send $\mathbf{C}_k^{t+1} = \mathcal{C}(\mathbf{H}_k(\mathbf{x}_k^{t+1}) - \mathbf{G}_k^t)$ to the server in parallel, for $k \in [K]$.
 - 4 Server sends $\nabla_k \Phi_{\mathcal{B}^t}(\mathbf{H}_{0\mathcal{B}^t}(\mathbf{x}_0^t), \{\mathbf{G}_{j\mathcal{B}^t}^t\}_{j=1}^K)$ to client k , in parallel, for $k \in \{0, 1, \dots, K\}$.
 - 5 Update $\mathbf{G}_k^{t+1} = \mathbf{G}_k^t + \mathbf{C}_k^{t+1}$ in parallel, for $k \in \{0, 1, \dots, K\}$.
-

We summarize the adaption of the EF-VFL method to the private labels setting in Algorithm 2.

Allowing for private labels broadens the range of applications for our method, since many VFL applications require not only private features, but also private labels, rendering any method requiring public labels inapplicable. However, as we will see in Section 5.2, using surrogate (5) instead of (4) can slow down convergence. Further, unlike Algorithm 1, which can be easily extendable to allow for multiple local updates at the clients between rounds of communication, Algorithm 2 works only for a single local update. This is because, for an VFL algorithm to perform multiple local updates, ϕ_n and \mathbf{x}_0 must be available at the clients, so that the forward and backward passes over the server model and the loss function can be performed locally after each update.

4 Convergence guarantees

In this section, we provide convergence guarantees for EF-VFL. We present our results for Algorithm 1 only, rather than stating them again for Algorithm 2, since they exhibit only a minor difference in Lemma 1 and in the main theorem, where the constant K is replaced with $K + 1$. We defer the details to Appendix A.

First, let us define the following sigma-algebra

$$\mathcal{F}_t := \sigma(\mathbf{G}^0, \mathbf{x}^1, \mathbf{G}^1, \dots, \mathbf{x}^t, \mathbf{G}^t),$$

where $\mathbf{G}^t := \{\mathbf{G}_0^t, \dots, \mathbf{G}_K^t\}$. For the sake of conciseness, we further let $\mathbb{E}_{\mathcal{F}}$ denote the conditional expectation $\mathbb{E}[\cdot | \mathcal{F}]$ with sigma-algebra \mathcal{F} . We use the following assumptions on our stochastic update vector $\tilde{\mathbf{g}}^t$ and the use of mini-batches.

Assumption 3 (Unbiased). *We assume that our stochastic update vector is unbiased:*

$$\forall(\mathbf{x}, t) \in \mathbb{R}^d \times \{0, 1, \dots, T - 1\}: \quad \mathbb{E}_{\mathcal{F}_t}[\tilde{\mathbf{g}}^t] = \mathbf{g}^t. \quad (\text{A3})$$

Assumption 4 (Bounded variance). *We assume that there exists a constant $\sigma \geq 0$ such that*

$$\forall(\mathbf{x}, t) \in \mathbb{R}^d \times \{0, 1, \dots, T - 1\}: \quad \mathbb{E}_{\mathcal{F}_t} \|\tilde{\mathbf{g}}^t - \mathbf{g}^t\|^2 \leq \frac{\sigma^2}{B}. \quad (\text{A4})$$

We now present Lemma 1 and Lemma 2, which we will use to prove our main theorems. We let $D^{(t)} := \sum_{k=0}^K \|\mathbf{G}_k^t - \mathbf{H}_k(\mathbf{x}_k^t)\|^2$ denote the total distortion (caused by compression) at time t .

Lemma 1 (Surrogate offset bound). *If Φ is L -smooth (A1) and $\{\mathbf{H}_k\}$ have bounded derivatives (A2), then, for all $t \geq 0$,*

$$\|\mathbf{g}^t - \nabla f(\mathbf{x}^t)\|^2 \leq KH^2L^2D^{(t)}. \quad (6)$$

Proof. See Appendix B.1. □

Lemma 2 (Recursive distortion bound). *Let $\{\mathbf{x}^t\}$ be a sequence generated by Algorithm 1. If \mathcal{C} is a contractive compressor (2), $\{\mathbf{H}_k\}$ have bounded derivatives (A2), and (A3) and (A4) hold, then, for all $t \geq 0$ and $\epsilon > 0$:*

$$\begin{aligned} \mathbb{E}D^{(t+1)} &\leq (1 - \alpha)(1 + \epsilon)\mathbb{E}D^{(t)} \\ &\quad + (1 - \alpha)(1 + \epsilon^{-1})\eta^2H^2 \left(\mathbb{E}\|\mathbf{g}^t\|^2 + \frac{\sigma^2}{B} \right). \end{aligned} \quad (7)$$

Proof. See Appendix B.2. □

4.1 Nonconvex setting

We now present our main convergence result for EF-VFL.

Theorem 1. *Let $\{\mathbf{x}^t\}$ be a sequence generated by Algorithm 1, \mathcal{C} be a contractive compressor (2), and $f^* > -\infty$. If (A1) to (A4) hold, then, for $0 < \eta \leq 1/(\sqrt{\rho_{\alpha 1}}L + L)$:*

$$\frac{1}{T} \sum_{t=0}^{T-1} \mathbb{E} \|\nabla f(\mathbf{x}^t)\|^2 \leq \frac{2\Delta}{\eta T} + (1 + \eta L \rho_{\alpha 1}) \frac{\eta L \sigma^2}{B} + \rho_{\alpha 2} \frac{\mathbb{E}D^{(0)}}{T}, \quad (8)$$

where the expectation is over the randomness in \mathcal{C} and in $\{\mathcal{B}_t\}$, $\Delta := f(\boldsymbol{\theta}^0) - f^*$, and

$$\rho_{\alpha 1} := KH^4 \left(\frac{1 + \sqrt{1 - \alpha}}{\alpha} - 1 \right)^2 \quad \text{and} \quad \rho_{\alpha 2} := \frac{KH^2L^2}{1 - \sqrt{1 - \alpha}}.$$

Proof. See Appendix C.1. □

If the batch size is large enough, $B = \Omega(\sigma^2/\delta)$, the iteration complexity to reach $\frac{1}{T} \sum_{t=0}^{T-1} \mathbb{E} \|\nabla f(\boldsymbol{\theta}^t)\|^2 \leq \delta$ matches the $\mathcal{O}(1/T)$ rate of the centralized, uncompressed setting. Also, in the absence of compression ($\alpha = 1$ and $D^{(t)} = 0$), we recover that, for $\eta \in (0, 1/L]$, we can output an \mathbf{x}^{out} such that $\mathbb{E} \|\nabla f(\mathbf{x}^{\text{out}})\|^2 \leq \frac{2\Delta}{\eta T} + \frac{\eta L \sigma^2}{B}$. If we are also in the full-batch case ($\sigma = 0$), we recover the gradient descent bound exactly: $\mathbb{E} \|\nabla f(\mathbf{x}^{\text{out}})\|^2 \leq \frac{2\Delta}{\eta T}$.

Note that, if we start our method by sending noncompressed representations (at $t = 0$ only), we can drop the last term in the upper bound in (8).

Our results improve over the prior state-of-the-art compressed vertical FL (CVFL) (Castiglia et al., 2022), whose convergence results for a fixed stepsize is presented below:

$$\frac{1}{T} \sum_{t=0}^{T-1} \mathbb{E} \|\nabla f(\mathbf{x}^t)\|^2 \leq \frac{4\Delta}{\eta T} + \mathcal{O}\left(\frac{\eta L \sigma^2}{B}\right) + \mathcal{O}\left(\frac{1}{T} \sum_{t=0}^{T-1} D_d^{(t)}\right).$$

Note how, even for full-batch updates, the upper bound above does not go to zero as $T \rightarrow \infty$ unless $D_d^{(t)} \rightarrow 0$, where $D_d^{(t)}$ is the distortion resulting from direct compression $D_d^{(t)} = \sum_{k=0}^K \|\mathcal{C}(\mathbf{H}_k(\mathbf{x}_k^t)) - \mathbf{H}_k(\mathbf{x}_k^t)\|^2$. That is, to achieve $\frac{1}{T} \sum_{t=0}^{T-1} \mathbb{E} \|\nabla f(\mathbf{x}^t)\|^2 \rightarrow 0$, CVFL requires a vanishing compression error, which necessitates that $\alpha \rightarrow 1$. This means that, despite reducing the total amount communications across the training, CVFL does not reduce the maximum amount of communications per round. In contrast, by allowing for nonvanishing compression, EF-VFL ensures small communication cost at every round.

4.2 Under the PL inequality

In this section, we establish the linear convergence of EF-VFL under the PL inequality (Polyak, 1963).

Assumption 5 (PL inequality). *We assume that there exists a positive constant μ such that*

$$\forall \mathbf{x} \in \mathbb{R}^d: \quad \|\nabla f(\mathbf{x})\|^2 \geq 2\mu(f(\mathbf{x}) - f^*). \quad (\text{A5})$$

We resort to the following Lyapunov function to show linear convergence:

$$V_t := \mathbb{E}f(\mathbf{x}^t) - f^* + c\mathbb{E}D^{(t)}, \quad (9)$$

where c is a positive constant. We now present Theorem 2.

Theorem 2. *Let $\{\mathbf{x}^t\}$ be a sequence generated by Algorithm 1, \mathcal{C} be a contractive compressor (2), and $f^* > -\infty$. If (A1) to (A5) hold, then, for η such that $\eta^2L^2(1 - \mu/L) + \eta\mu \leq \alpha^2$, we have:*

$$V_T \leq (1 - \eta\mu)^T V_0 + \frac{\sigma^2}{2B\mu}.$$

Table 1: Total communication cost to reach error level $\delta > 0$ (top- k ; full-batch; single local update).

\mathcal{C}	SVFL [19]	CVFL [12]	EF-VFL (ours)	EF-VFL with private labels (ours)
Uplink (total)	$N\bar{E}K \cdot \mathcal{O}(1/\delta)$	$\min\{k \cdot \mathcal{O}(1/\sqrt{\delta}), N\bar{E}\} \cdot K \cdot \mathcal{O}(1/\delta^2)$	$kK \cdot \mathcal{O}(1/\delta)$	$kK \cdot \mathcal{O}(1/\delta)$
Downlink (total/broadcast)	$N\bar{E}K \cdot \mathcal{O}(1/\delta)$	$\min\{k \cdot \mathcal{O}(1/\sqrt{\delta}), N\bar{E}\} \cdot (K+1) \cdot \mathcal{O}(1/\delta^2)$	$k(K+1) \cdot \mathcal{O}(1/\delta)$	$kK \cdot \mathcal{O}(1/\delta)$

Proof. See Appendix C.2. □

Since $\mu \leq L$, we have that $\eta \in (0, 1/L)$ implies that $1 - \eta\mu \in (0, 1)$. Hence, EF-VFL converges linearly to a $\mathcal{O}(\sigma^2)$ neighborhood around the global optimum.

In Table 1, where $\bar{E} = E_j$ for $j \in [K]$ is the embedding size for each sample at each client (assumed to match for simplicity), we present the total communication cost to reach $\frac{1}{T} \sum_{t=0}^{T-1} \mathbb{E} \|\nabla f(\boldsymbol{\theta}^t)\|^2 \leq \delta$, where $\delta > 0$ (top- k ; full-batch; single local update). We discuss different downlink communication schemes for EF-VFL in Appendix D.

5 Experiments

We compare EF-VFL with two baselines: **(1)** standard VFL (SVFL), which corresponds to the method in Liu et al. (2022) and is mathematically equivalent to stochastic gradient descent when a single local update is used, and **(2)** CVFL (Castiglia et al., 2022), which recovers SVFL when an identity compressor is used (that is, without employing compression). All of our results correspond to the mean and standard deviation for five different seeds. We employ two popular compressors in our experiments.

- Top- k sparsification (Alistarh et al., 2018; Stich et al., 2018) is a map $\text{top}_k: \mathbb{R}^d \mapsto \mathbb{R}^d$ defined as

$$\text{top}_k(\mathbf{v}) := \mathbf{v} \odot \mathbf{u}(\mathbf{v}),$$

where \odot denotes the Hadamard product and $\mathbf{u}(\mathbf{v})$ is such that its entry i is 1 if v_i is one of the k largest entries of \mathbf{v} in absolute value and 0 otherwise. We have that (2) holds for $\alpha = k/d$.

- Stochastic quantization (Alistarh et al., 2017) is a map $\text{qsgd}_s: \mathbb{R}^d \mapsto \mathbb{R}^d$, with $s > 1$ quantization levels defined as

$$\text{qsgd}_s(\mathbf{v}) := \frac{\|\mathbf{v}\| \cdot \text{sign}(\mathbf{v})}{s\tau} \cdot \left\lfloor s \frac{|\mathbf{v}|}{\|\mathbf{v}\|} + \xi \right\rfloor,$$

where $\tau = 1 + \min\{d/s^2, \sqrt{d}/s\}$ and $\xi \sim \mathcal{U}([0, 1]^d)$, where \mathcal{U} denotes the uniform distribution. In practice, we are interested in values of s such that $s = 2^b$, where b is the number of bits. We have that (2) holds for $\alpha = 1/\tau$.

For the sake of the comparison with CVFL, we employ compressors $\mathcal{C} = \mathcal{C}_2 \circ \mathcal{C}_1$, where \mathcal{C}_2 is either $\text{top}_k(\mathbf{v})$ or qsgd_s and \mathcal{C}_1 selects the rows in \mathcal{B}^t , similarly to CVFL. Further, as explained in Section 3, our experiments focus on the compression of $\{\mathbf{H}_k(\mathbf{x}_k)\}_{k=1}^K$, and not \mathbf{x}_0 .

5.1 Comparison with SVFL and CVFL

The detailed hyperparameters for the following experiments can be found in the provided code.

MNIST. We train a shallow neural network (one hidden layer) on the MNIST digit recognition dataset (Le-Cun et al., 1998). The 28×28 images in the original dataset \mathcal{D} are split into four local datasets \mathcal{D}_k of 14×14 images, its quadrants ($K = 4$). The local models \mathbf{h}_{kn} are maps $\mathbf{v} \mapsto \text{sigmoid}(\mathbf{W}_{k1}\mathbf{v})$, with $\mathbf{W}_{k1} \in \mathbb{R}^{128 \times 196}$, and the server model is $(\mathbf{v}_1, \dots, \mathbf{v}_4) \mapsto \mathbf{W}_2(\sum_{k=1}^4 \mathbf{v}_k)$, with $\mathbf{W}_2 \in \mathbb{R}^{10 \times 16}$. We use cross-entropy loss. In Figure 2, we present the results for when EF-VFL and CVFL employ top_k , keeping 10%, 1%, and 0.1% of the entries, and when they employ qsgd_s , sending $b \in \{4, 2, 1\}$ bits per entry, instead of the uncompressed $b = 32$. In both figures, we see that EF-VFL outperforms SVFL and CVFL in communication efficiency. In terms of results per epoch, EF-VFL significantly outperforms CVFL and, for a sufficiently large k (for top_k) or b (for

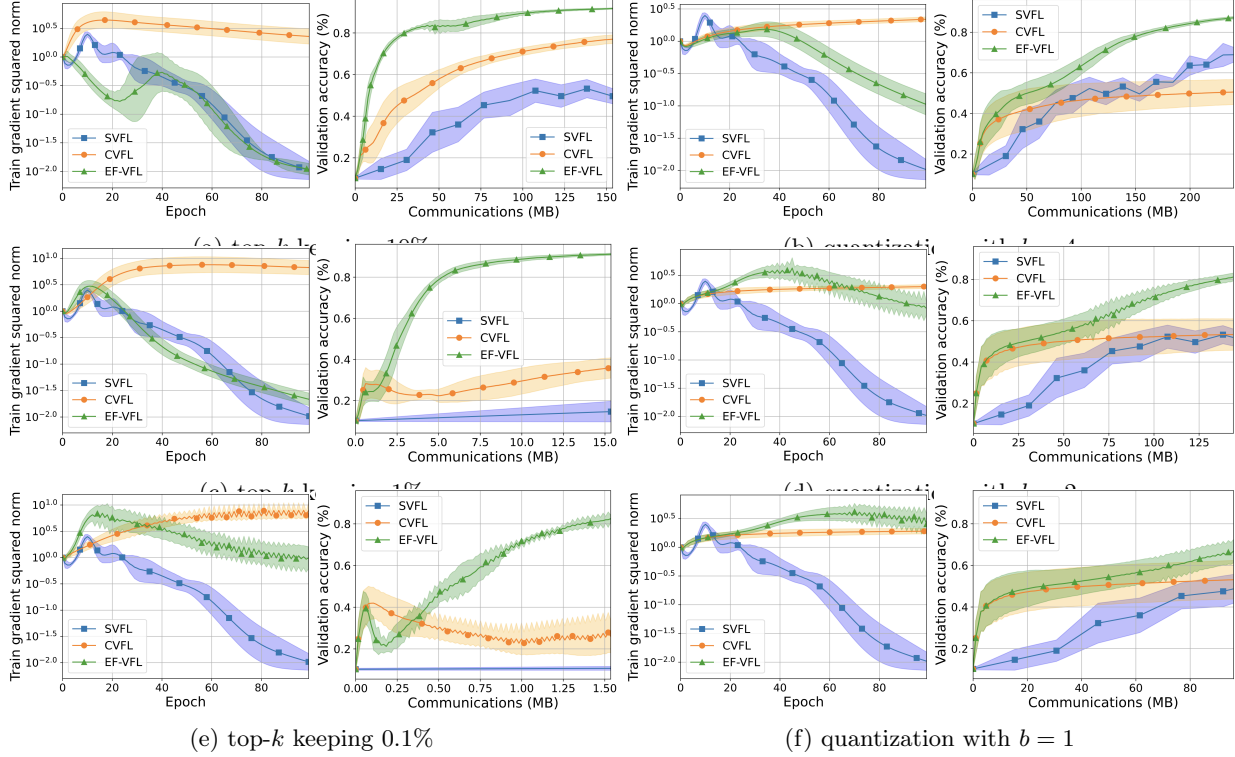


Figure 2: The (relative) training gradient squared norm with respect to epochs and validation accuracy with respect to communication cost for the training of a shallow neural network on MNIST. On the left, CVFL and EF-VFL employ top- k sparsification with a decreasing k across rows. On the right, they employ stochastic quantization with a decreasing number of bits across rows. SVFL is the same throughout.

qsgd_s) EF-VFL achieves a similar performance to SVFL. As predicted in Section 4, the train gradient squared norm during training goes to zero for EF-VFL, as it does for SVFL, but not for CVFL.

ModelNet10. We train a multi-view convolutional neural network (MVCNN) (Su et al., 2015) on ModelNet10 (Wu et al., 2015), a dataset of three-dimensional CAD models. We use a preprocessed version of ModelNet10, where each sample is represented by 12 two-dimensional views. We assign a view per client ($K = 12$). In Figure 3, we present the results for when EF-VFL and CVFL employ top _{k} , keeping 20%, 2%, and 0.2% of the entries, and when they employ qsgd_s, with $b \in \{8, 4, 2\}$. We plot the train loss with respect to the number of epochs and the validation accuracy with respect to the communication cost. We observe that, for EF-VFL, the training loss decreases more rapidly than for CVFL. Further, if the compression is not excessively aggressive, EF-VFL performs similarly to SVFL. In terms of communication efficiency, EF-VFL outperforms both SVFL and CVFL.

CIFAR-100. We train a model based on a residual neural network, ResNet18 (He et al., 2016), on CIFAR-100 (Krizhevsky et al., 2009). More precisely, we divide each image into four quadrants and allocate one quadrant to each client ($K = 4$), with each client using a ResNet18 model as its local model. The server model is linear (a single layer). In Figure 4, we present the results for when EF-VFL and CVFL employ top _{k} , keeping 10%, 1%, and 0.1% of the entries, and when they employ qsgd_s, with $b \in \{4, 2, 1\}$. We plot the train loss with respect to the number of epochs and the validation accuracy with respect to the communication cost. Regarding the results with respect to the number of epochs, EF-VFL achieves a similar performance to that of SVFL, significantly outperforming CVFL. In terms of communication efficiency, EF-VFL outperforms both SVFL and CVFL.

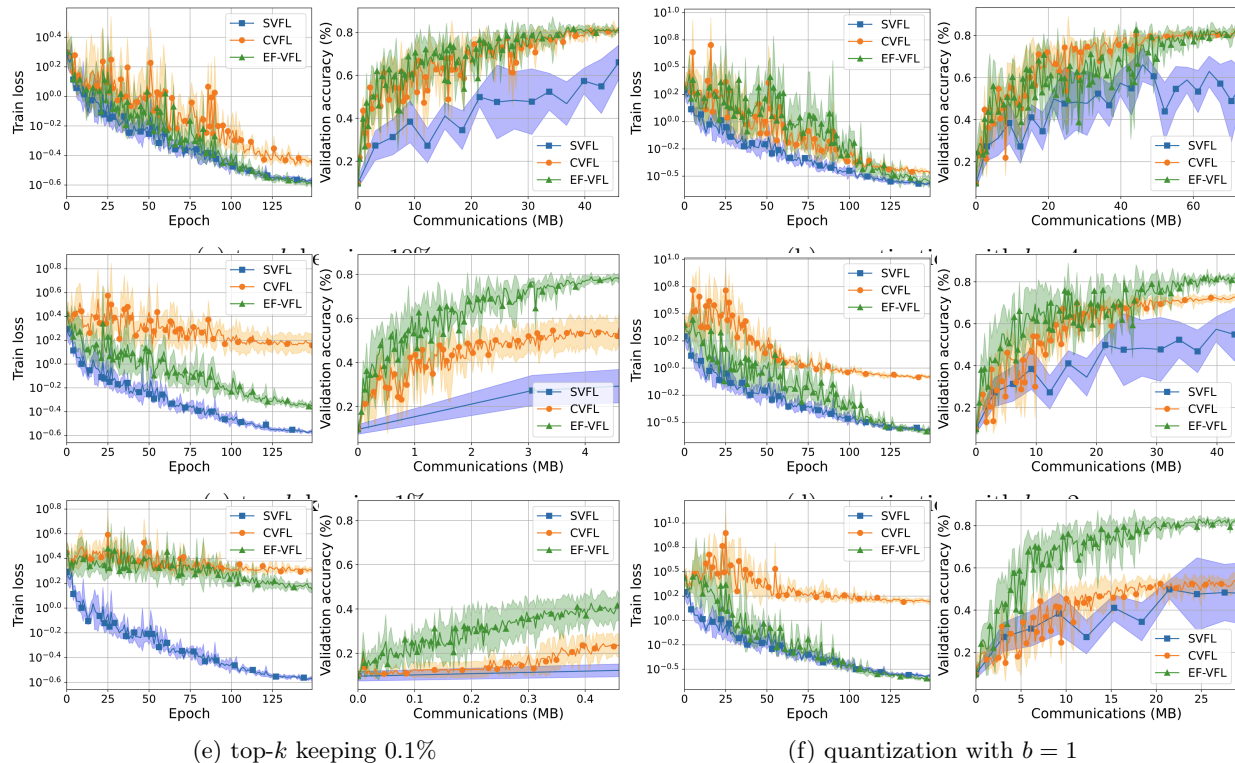


Figure 3: Train loss with respect to the number of epochs and validation accuracy with respect to the communication cost for the training of an MVCNN on ModelNet10. On the left, CVFL and EF-VFL employ top- k sparsification with a decreasing k across rows. On the right, they employ stochastic quantization with a decreasing number of bits across rows. SVFL is the same throughout.

We summarize the test metrics for all three tasks in Table 2. In brief, while CVFL performs well for less aggressive compression is employed, the improved performance of EF-VFL is significant when more aggressive compression is employed.

5.2 Performance under private labels

In this section, we run experiments on the adaption of EF-VFL to handle private labels, proposed in Section 3.1.

In Castiglia et al. (2022), the authors assume that the labels are available at all clients and do not propose an adaptation of CVFL to deal with private labels. Yet, to get a baseline for a compressed VFL method allowing for label privacy, we adapt CVFL in a similar manner to how we adapt EF-VFL (that is, sending back the derivative from the server to the clients, instead of ϕ_n and \mathbf{x}_0 , and without backpropagating through the compression operator).

We run an experiment on MNIST, training the same shallow neural network as in model as in Section 5.1, with all the same settings, except for the use of batch size $B = 1024$. Further, we train a ResNet18-based model with a linear server model (a single layer) on CIFAR-100 (Krizhevsky et al., 2009). For all the optimizers, we use an initial stepsize of $\eta = 0.01$ and a cosine annealing scheduler with a minimum stepsize of $1/100$ the initial value and use a batch size $B = 128$ and a weight decay of 0.01. The compressed-communication methods employ top- k , keeping 5% of the entries.

In Figure 5, we observe that, although the modified EF-VFL for handling private labels converges noticeably slower than the original method, it still performs effectively. For both the MNIST experiment and the CIFAR-100 experiment, we see that, while adapting CVFL to handle private labels leads to a severe drop in performance, EF-VFL slows down much less noticeably. In fact, for the MNIST experiment, EF-VFL with private labels still outperforms CVFL, even with public labels.

Table 2: Test accuracy for SVFL, CVFL, and EF-VFL across different tasks, for a fixed number of epochs. We run reach experiment for 5 seeds and present the mean accuracy \pm standard deviation, highlighting the highest accuracy in bold.

MNIST (accuracy, %)							
	Uncompressed	top- k compressor			qsgd compressor		
		keep 10%	keep 1%	keep 0.1%	$b = 4$	$b = 2$	$b = 1$
SVFL	91.6 \pm 0.1	—	—	—	—	—	—
CVFL	—	77.2 \pm 1.9	35.7 \pm 5.0	25.7 \pm 7.6	50.3 \pm 6.1	53.0 \pm 7.4	52.7 \pm 8.7
EF-VFL	—	91.8 \pm 0.1	91.1 \pm 0.3	82.4 \pm 2.1	87.2 \pm 0.4	81.1 \pm 1.6	66.8 \pm 5.9
ModelNet10 (accuracy, %)							
	Uncompressed	top- k compressor			qsgd compressor		
		keep 10%	keep 1%	keep 0.1%	$b = 4$	$b = 2$	$b = 1$
SVFL	81.2 \pm 0.8	—	—	—	—	—	—
CVFL	—	80.7 \pm 3.1	53.2 \pm 6.5	24.5 \pm 4.2	80.3 \pm 2.0	70.7 \pm 1.6	52.0 \pm 3.2
EF-VFL	—	80.4 \pm 1.9	77.4 \pm 2.5	40.3 \pm 4.8	79.4 \pm 3.7	80.4 \pm 2.7	81.1 \pm 2.8
CIFAR-100 (accuracy, %)							
	Uncompressed	top- k compressor			qsgd compressor		
		keep 10%	keep 1%	keep 0.1%	$b = 4$	$b = 2$	$b = 1$
SVFL	57.7 \pm 0.6	—	—	—	—	—	—
CVFL	—	56.8 \pm 0.6	45.1 \pm 2.3	11.6 \pm 1.4	19.2 \pm 0.6	5.9 \pm 0.7	2.0 \pm 0.1
EF-VFL	—	57.2 \pm 0.8	54.8 \pm 0.9	36.4 \pm 2.8	57.8 \pm 0.5	50.2 \pm 1.3	34.7 \pm 2.8

5.3 Performance under multiple local updates

As mentioned earlier, some VFL works employ $Q > 1$ local updates per round (Liu et al., 2022), using stale information from the other machines. We now show that, although our analysis focuses on the case where each client performs a single local update at each round of communications (that is, $Q = 1$), EF-VFL performs well in the $Q > 1$ case too. In particular, to study the performance of EF-VFL when carrying out multiple local updates, we train an MVCNN on ModelNet10 and a ResNet18 on CIFAR-10.

For ModelNet10, all three VFL optimizers use a batch size $B = 128$, a stepsize $\eta = 0.004$, and a weight decay of 0.01. Further, we use a learning rate scheduler, halving the learning rate at epochs 50 and 75. The results are presented in Figure 6a and Figure 6b. For CIFAR-10, all three VFL optimizers use a batch size $B = 128$, a stepsize $\eta = 0.0025$, and a weight decay of 0.01. Further, we use a learning rate scheduler, halving the learning rate at epochs 40, 60, and 80. The results are presented in Figure 6c and Figure 6d.

For both ModelNet10 and CIFAR-10, we see that, similarly to the $Q = 1$ case, our method outperforms SVFL and CVFL in communication efficiency. In terms of results per epoch, EF-VFL performs similarly to SVFL and significantly better than CVFL. Interestingly, for the CIFAR-10 task, EF-VFL even outperforms SVFL with respect to the number of epochs. We suspect this may be due to the fact that compression helps to mitigate the overly greedy nature of the parallel updates based on stale information.

6 Conclusions

In this work, we proposed EF-VFL, a method for compressed vertical federated learning. Our method leverages an error feedback mechanism to achieve a $\mathcal{O}(1/T)$ convergence rate for a sufficiently large batch size, improving upon the state-of-the-art rate of $\mathcal{O}(1/\sqrt{T})$. Numerical experiments further demonstrate the faster convergence of our method. We further show that, under the PL inequality, our method converges linearly and introduce a modification of EF-VFL supporting the use of private labels. In the future, it would be interesting to study the use of error feedback based compression methods for VFL in the fully-decentralized and semi-decentralized settings, in setups with asynchronous updates, and in combination with privacy mechanisms, such as differential privacy as done in the horizontal setting (Li et al., 2022; Li and Chi, 2023).

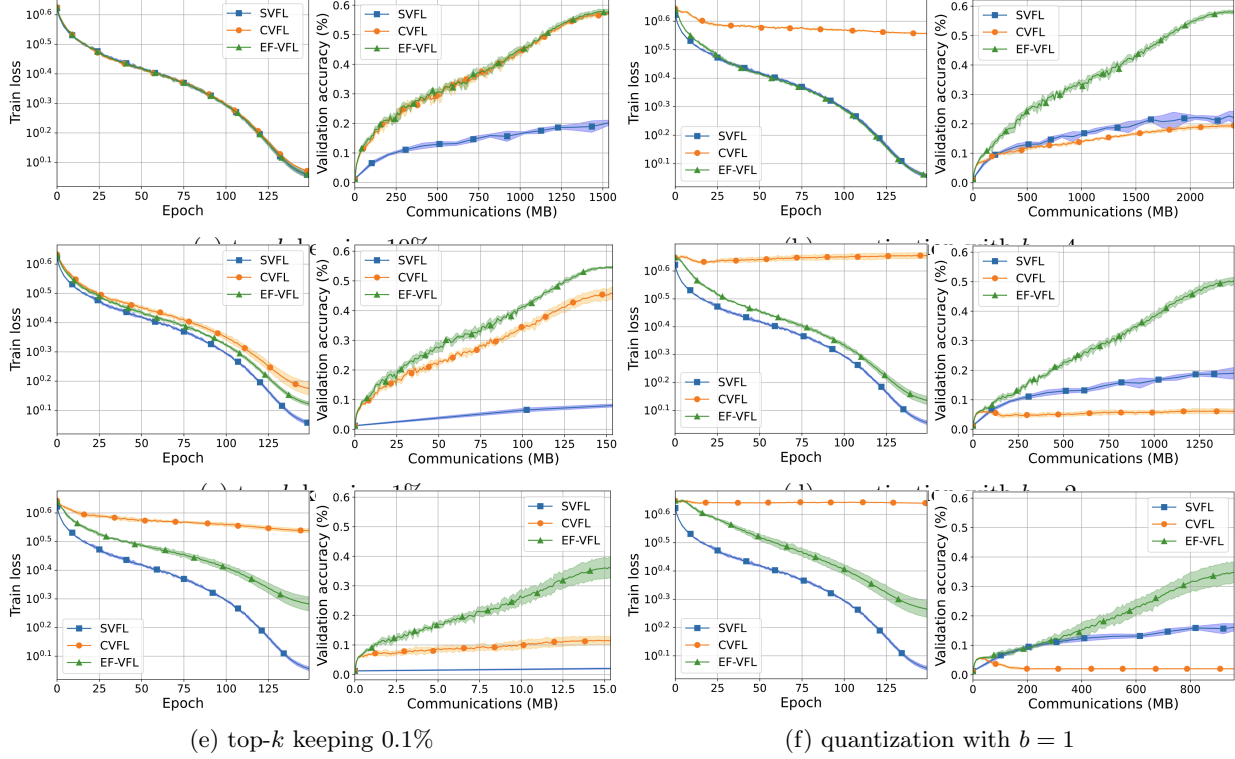


Figure 4: Train loss with respect to the number of epochs and the validation accuracy with respect to the communication cost for the training of a ResNet18-based model on CIFAR-100. On the left, CVFL and EF-VFL employ top- k sparsification with a decreasing k across rows. On the right, they employ stochastic quantization with a decreasing number of bits across rows. SVFL is the same throughout.

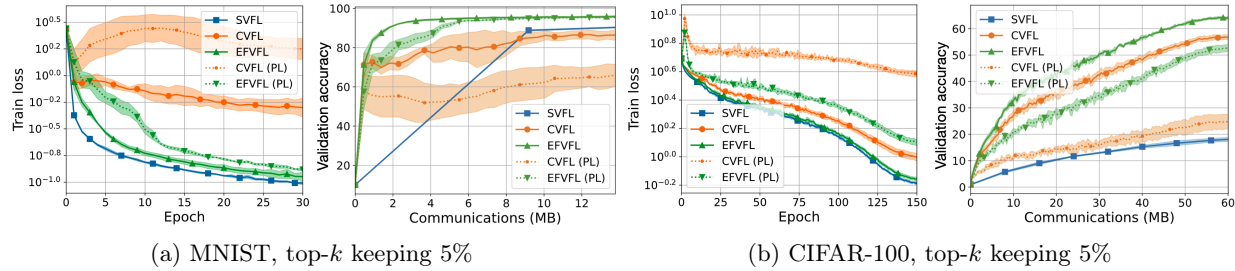


Figure 5: Train loss with respect to the number of epochs and validation accuracy with respect to the communication cost for the training of a shallow neural network on MNIST and a ResNet18-based model on CIFAR-100. In the legend, PL stands for private labels. The communication compressed methods—CVFL, EF-VFL, CVFL (PL), and EF-VFL (PL)—employ top- k sparsification.

Acknowledgements

This work is supported in part by the Fundação para a Ciência e a Tecnologia through the Carnegie Mellon Portugal Program; by the grants U.S. National Science Foundation CCF-2007911 and ECCS-2318441; by the CMU-Portugal project CMU/TIC/0016/2021; by NOVA LINC funding (DOI: 10.54499/UIDB/04516/2020 and 10.54499/UIDP/04516/2020); by LARSyS FCT funding (DOI: 10.54499/LA/P/0083/2020); by PT Smart Retail project [PRR - 02/C05-i11/2024.C645440011-00000062], through IAPMEI - Agência para a Competitividade e Inovação; and by TaRDIS Horizon2020 Contract ID: 101093006.

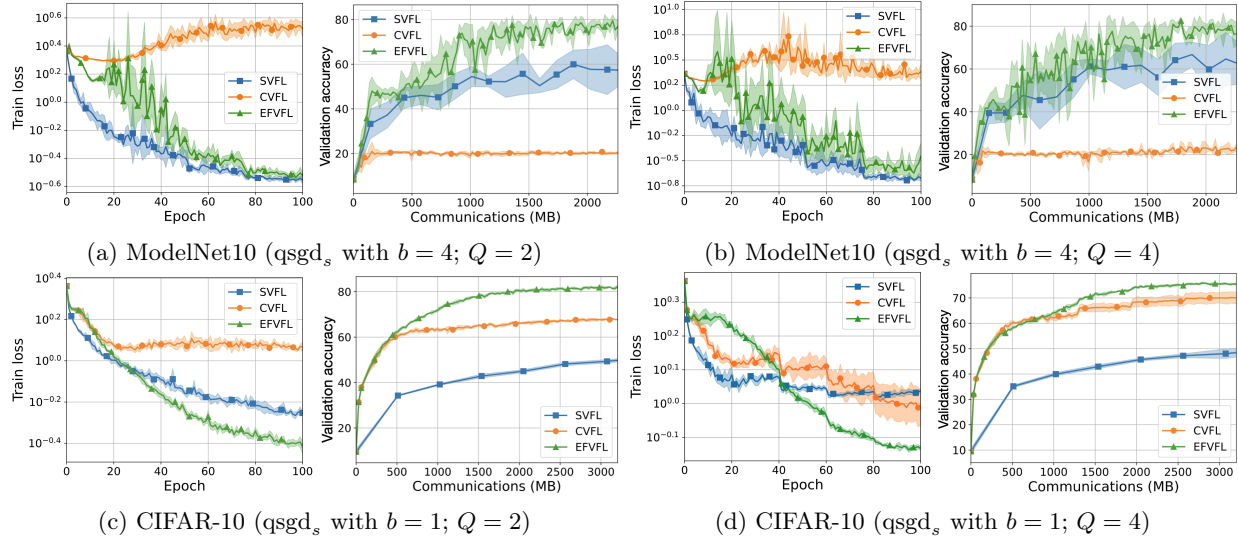


Figure 6: Train loss with respect to the number of epochs and validation accuracy with respect to the communication cost for the training of a multi-view convolutional neural network on ModelNet10 and a residual neural network on CIFAR-10. CVFL and EF-VFL use stochastic quantization. On the left, all three vertical FL optimizers use $Q = 2$ local updates and, on the right, they all use $Q = 4$ local updates.

References

- D. Alistarh, D. Grubic, J. Li, R. Tomioka, and M. Vojnovic. QSGD: Communication-efficient SGD via gradient quantization and encoding. *Advances in neural information processing systems*, 30, 2017.
- D. Alistarh, T. Hoeffler, M. Johansson, N. Konstantinov, S. Khirirat, and C. Renggli. The convergence of sparsified gradient methods. *Advances in Neural Information Processing Systems*, 31, 2018.
- M. M. Amiri and D. Gündüz. Machine learning at the wireless edge: Distributed stochastic gradient descent over-the-air. *IEEE Transactions on Signal Processing*, 68:2155–2169, 2020.
- A. Beznosikov, S. Horváth, P. Richtárik, and M. Safaryan. On biased compression for distributed learning. *Journal of Machine Learning Research*, 24(276):1–50, 2023.
- T. Castiglia, S. Wang, and S. Patterson. Flexible vertical federated learning with heterogeneous parties. *IEEE Transactions on Neural Networks and Learning Systems*, 2023.
- T. J. Castiglia, A. Das, S. Wang, and S. Patterson. Compressed-VFL: Communication-efficient learning with vertically partitioned data. In *International Conference on Machine Learning*, pages 2738–2766. PMLR, 2022.
- I. Ceballos, V. Sharma, E. Mugica, A. Singh, A. Roman, P. Vepakomma, and R. Raskar. SplitNN-driven vertical partitioning. *arXiv:2008.04137*, 2020.
- J. Chen and A. H. Sayed. Diffusion adaptation strategies for distributed optimization and learning over networks. *IEEE Transactions on Signal Processing*, 60(8):4289–4305, 2012.
- T. Chen, X. Jin, Y. Sun, and W. Yin. VAFI: a method of vertical asynchronous federated learning. *arXiv:2007.06081*, 2020.
- Y. Cheng, Y. Liu, T. Chen, and Q. Yang. Federated learning for privacy-preserving AI. *Communications of the ACM*, 63(12):33–36, 2020.
- J. Dean, G. Corrado, R. Monga, K. Chen, M. Devin, M. Mao, M. Ranzato, A. Senior, P. Tucker, K. Yang, et al. Large scale distributed deep networks. *Advances in neural information processing systems*, 25, 2012.

- Y. Du, S. Yang, and K. Huang. High-dimensional stochastic gradient quantization for communication-efficient edge learning. *IEEE transactions on signal processing*, 68:2128–2142, 2020.
- F. Haddadpour, M. M. Kamani, A. Mokhtari, and M. Mahdavi. Federated learning with compression: Unified analysis and sharp guarantees. In *International Conference on Artificial Intelligence and Statistics*, pages 2350–2358. PMLR, 2021.
- K. He, X. Zhang, S. Ren, and J. Sun. Deep residual learning for image recognition. In *Proceedings of the IEEE conference on computer vision and pattern recognition*, 2016.
- Y. Hu, D. Niu, J. Yang, and S. Zhou. Fdml: A collaborative machine learning framework for distributed features. In *Proceedings of the 25th ACM SIGKDD International Conference on Knowledge Discovery & Data Mining*, pages 2232–2240, 2019.
- H. Inose, Y. Yasuda, and J. Murakami. A telemetering system by code modulation- δ - σ modulation. *IRE Transactions on Space Electronics and Telemetry*, (3):204–209, 1962.
- S. P. Karimireddy, Q. Rebjock, S. Stich, and M. Jaggi. Error feedback fixes signsgd and other gradient compression schemes. In *International Conference on Machine Learning*, pages 3252–3261. PMLR, 2019.
- A. Khan, M. ten Thij, and A. Wilbik. Communication-efficient vertical federated learning. *Algorithms*, 15(8): 273, 2022.
- A. Koloskova, S. Stich, and M. Jaggi. Decentralized stochastic optimization and gossip algorithms with compressed communication. In *International Conference on Machine Learning*, pages 3478–3487. PMLR, 2019.
- A. Krizhevsky, G. Hinton, et al. Learning multiple layers of features from tiny images. 2009.
- Y. LeCun, L. Bottou, Y. Bengio, and P. Haffner. Gradient-based learning applied to document recognition. *Proceedings of the IEEE*, 86(11):2278–2324, 1998.
- B. Li and Y. Chi. Convergence and privacy of decentralized nonconvex optimization with gradient clipping and communication compression. *arXiv preprint arXiv:2305.09896*, 2023.
- M. Li, Y. Chen, Y. Wang, and Y. Pan. Efficient asynchronous vertical federated learning via gradient prediction and double-end sparse compression. In *2020 16th international conference on control, automation, robotics and vision (ICARCV)*, pages 291–296. IEEE, 2020.
- Z. Li, H. Zhao, B. Li, and Y. Chi. SoteriaFL: A unified framework for private federated learning with communication compression. *Advances in Neural Information Processing Systems*, 35:4285–4300, 2022.
- X. Lian, C. Zhang, H. Zhang, C.-J. Hsieh, W. Zhang, and J. Liu. Can decentralized algorithms outperform centralized algorithms? A case study for decentralized parallel stochastic gradient descent. *Advances in Neural Information Processing Systems*, 30, 2017.
- Y. Liu, X. Zhang, Y. Kang, L. Li, T. Chen, M. Hong, and Q. Yang. FedBCD: A communication-efficient collaborative learning framework for distributed features. *IEEE Transactions on Signal Processing*, 70: 4277–4290, 2022.
- Y. Liu, Y. Kang, T. Zou, Y. Pu, Y. He, X. Ye, Y. Ouyang, Y.-Q. Zhang, and Q. Yang. Vertical federated learning: Concepts, advances, and challenges. *IEEE Transactions on Knowledge and Data Engineering*, 2024.
- B. McMahan, E. Moore, D. Ramage, S. Hampson, and B. A. y Arcas. Communication-efficient learning of deep networks from decentralized data. In *Artificial intelligence and statistics*, pages 1273–1282. PMLR, 2017.
- K. Mishchenko, E. Gorbunov, M. Takáč, and P. Richtárik. Distributed learning with compressed gradient differences. *Optimization Methods and Software*, pages 1–16, 2024.

- J. F. Mota, J. M. Xavier, P. M. Aguiar, and M. Püschel. D-admm: A communication-efficient distributed algorithm for separable optimization. *IEEE Transactions on Signal processing*, 61(10):2718–2723, 2013.
- R. Nassif, S. Vlaski, M. Carpentiero, V. Matta, M. Antonini, and A. H. Sayed. Quantization for decentralized learning under subspace constraints. *IEEE Transactions on Signal Processing*, 71:2320–2335, 2023.
- B. T. Polyak. Gradient methods for the minimisation of functionals. *USSR Computational Mathematics and Mathematical Physics*, 3(4):864–878, 1963.
- P. Richtárik, I. Sokolov, and I. Fatkhullin. EF21: A new, simpler, theoretically better, and practically faster error feedback. *Advances in Neural Information Processing Systems*, 34:4384–4396, 2021.
- A. Sapio, M. Canini, C.-Y. Ho, J. Nelson, P. Kalnis, C. Kim, A. Krishnamurthy, M. Moshref, D. Ports, and P. Richtárik. Scaling distributed machine learning with in-network aggregation. In *18th USENIX Symposium on Networked Systems Design and Implementation (NSDI 21)*, pages 785–808, 2021.
- F. Seide, H. Fu, J. Droppo, G. Li, and D. Yu. 1-bit stochastic gradient descent and its application to data-parallel distributed training of speech dnns. In *Fifteenth annual conference of the international speech communication association*, 2014.
- T. Sery, N. Shlezinger, K. Cohen, and Y. C. Eldar. Over-the-air federated learning from heterogeneous data. *IEEE Transactions on Signal Processing*, 69:3796–3811, 2021.
- N. Shlezinger, M. Chen, Y. C. Eldar, H. V. Poor, and S. Cui. Uveqfed: Universal vector quantization for federated learning. *IEEE Transactions on Signal Processing*, 69:500–514, 2020.
- S. U. Stich, J.-B. Cordonnier, and M. Jaggi. Sparsified SGD with memory. *Advances in Neural Information Processing Systems*, 31, 2018.
- H. Su, S. Maji, E. Kalogerakis, and E. Learned-Miller. Multi-view convolutional neural networks for 3D shape recognition. In *Proceedings of the IEEE international conference on computer vision*, 2015.
- P. Valdeira, Y. Chi, C. Soares, and J. Xavier. A multi-token coordinate descent method for semi-decentralized vertical federated learning. *arXiv:2309.09977*, 2023.
- P. Valdeira, J. Xavier, C. Soares, and Y. Chi. Communication-efficient vertical federated learning via compressed error feedback. *32nd European Signal Processing Conference (EUSIPCO)*, 2024.
- Z. Wu, S. Song, A. Khosla, F. Yu, L. Zhang, X. Tang, and J. Xiao. 3D ShapeNets: A deep representation for volumetric shapes. In *Proceedings of the IEEE conference on computer vision and pattern recognition*, 2015.
- C. Xie, S. Koyejo, and I. Gupta. Asynchronous federated optimization. *arXiv:1903.03934*, 2019.
- L. Yang, D. Chai, J. Zhang, Y. Jin, L. Wang, H. Liu, H. Tian, Q. Xu, and K. Chen. A survey on vertical federated learning: From a layered perspective. *arXiv:2304.01829*, 2023.
- B. Ying, K. Yuan, and A. H. Sayed. Supervised learning under distributed features. *IEEE Transactions on Signal Processing*, 67(4):977–992, 2018.
- X. Zhang, M. Hong, S. Dhople, W. Yin, and Y. Liu. Fedpd: A federated learning framework with adaptivity to non-iid data. *IEEE Transactions on Signal Processing*, 69:6055–6070, 2021.
- H. Zhao, B. Li, Z. Li, P. Richtárik, and Y. Chi. Beer: Fast $O(1/T)$ rate for decentralized nonconvex optimization with communication compression. *Advances in Neural Information Processing Systems*, 35: 31653–31667, 2022.

A Preliminaries

If a function is L -smooth (A1), then the following quadratic upper bound holds:

$$\forall \mathbf{x}, \mathbf{y} \in \mathbb{R}^d: \quad f(\mathbf{y}) \leq f(\mathbf{x}) + \nabla f(\mathbf{x})^\top (\mathbf{y} - \mathbf{x}) + \frac{L}{2} \|\mathbf{x} - \mathbf{y}\|^2. \quad (10)$$

It follows from Assumption (2) that the following inequality holds:

$$\|\mathbf{H}_k(\mathbf{x}) - \mathbf{H}_k(\mathbf{y})\| \leq H \|\mathbf{x} - \mathbf{y}\|, \quad \forall \mathbf{x}, \mathbf{y} \in \mathbb{R}^{d_k}. \quad (11)$$

Letting $\epsilon > 0$, we use the following standard inequality in our analysis:

$$\forall \mathbf{x}, \mathbf{y} \in \mathbb{R}^d: \quad \|\mathbf{x} + \mathbf{y}\|^2 \leq (1 + \epsilon) \|\mathbf{x}\|^2 + (1 + \epsilon^{-1}) \|\mathbf{y}\|^2. \quad (12)$$

We define the distortion associated with block k at time t as

$$D_k^{(t)} := \|\mathbf{G}_k^t - \mathbf{H}_k(\mathbf{x}_k^t)\|^2$$

and, recall, we denote the total distortion at time t as $D^{(t)} = \sum_{k=0}^K D_k^{(t)}$. We also define $\nu := (1 - \alpha) \in [0, 1)$.

In Section 4, we introduced the following sigma-algebra

$$\mathcal{F}_t = \sigma(\mathbf{G}^0, \mathbf{x}^1, \mathbf{G}^1, \dots, \mathbf{x}^t, \mathbf{G}^t),$$

where $\mathbf{G}^t = \{\mathbf{G}_0^t, \dots, \mathbf{G}_K^t\}$. We now further define

$$\mathcal{F}'_t := \sigma(\mathbf{G}^0, \mathbf{x}^1, \mathbf{G}^1, \dots, \mathbf{x}^t, \mathbf{G}^t, \mathbf{x}^{t+1}).$$

Recall that we let $\mathbb{E}_{\mathcal{F}}$ denote the conditional expectation $\mathbb{E}[\cdot \mid \mathcal{F}]$.

Note that, while we write our proofs for Algorithm 1, they can be easily adjusted to cover Algorithm 2. To do so, it suffices to adjust the notation, replacing \mathbf{g}^t and $\tilde{\mathbf{g}}^t$ by ∇_k^t and $\tilde{\nabla}_k^t$, respectively, and to make minor changes to the proof of Lemma 1, which cause the constant K in Lemma 1 to be replaced with $K + 1$. This, in turn, leads to a similar adjustment in the constants of our main theorems.

B Supporting Lemmas

B.1 Proof of Lemma 1

Decoupling the offset across blocks, we get that

$$\begin{aligned} \|\mathbf{g}^t - \nabla f(\mathbf{x}^t)\|^2 &= \sum_{k=0}^K \|\mathbf{g}_k^t - \nabla_k f(\mathbf{x}_k^t)\|^2, \\ &\leq \sum_{k=0}^K \|\nabla \mathbf{H}_k(\mathbf{x}_k^t)\|^2 \left\| \tilde{\nabla}_k^t \Phi - \nabla_k \Phi(\{\mathbf{H}_k(\mathbf{x}_k^t)\}_{k=0}^K) \right\|^2, \end{aligned}$$

where we use the chain rule and the fact that $\|\mathbf{A}\mathbf{x}\| \leq \|\mathbf{A}\| \|\mathbf{x}\|$. Now, it follows from the bounded gradient assumption (A2) on $\{\mathbf{H}_k\}$ and the L -smoothness (A1) of Φ that

$$\begin{aligned} \|\mathbf{g}^t - \nabla f(\mathbf{x}^t)\|^2 &\leq H^2 L^2 \sum_{k=0}^K \sum_{j \neq k} \|\mathbf{G}_j^t - \mathbf{H}_j(\mathbf{x}_j^t)\|^2 \\ &= H^2 L^2 \sum_{k=0}^K \sum_{j \neq k} D_j^{(t)} \\ &= KH^2 L^2 D^{(t)}, \end{aligned}$$

as we set out to prove. For Algorithm 2, the sum $\sum_{j \neq k}$ would instead be $\sum_{j=1}^K$, leading to $\|\mathbf{g}^t - \nabla f(\mathbf{x}^t)\|^2 \leq (K + 1)H^2 L^2 D^{(t)}$. However, note that, for Algorithm 2, $D_0^{(t)} = 0$.

B.2 Proof of Lemma 2

It follows from the definition of distortion and from the update of our compression estimate that

$$\begin{aligned}\mathbb{E}_{\mathcal{F}'_t} \left[D_k^{(t+1)} \right] &= \mathbb{E}_{\mathcal{F}'_t} \left\| \mathbf{G}_k^{t+1} - \mathbf{H}_k(\mathbf{x}_k^{t+1}) \right\|^2 \\ &= \mathbb{E}_{\mathcal{F}'_t} \left\| \mathbf{G}_k^t + \mathcal{C}(\mathbf{H}_k(\mathbf{x}_k^{t+1}) - \mathbf{G}_k^t) - \mathbf{H}_k(\mathbf{x}_k^{t+1}) \right\|^2.\end{aligned}$$

Now, from the definition of contractive compressor (2) and from (12), we have that

$$\begin{aligned}\mathbb{E}_{\mathcal{F}'_t} \left[D_k^{(t+1)} \right] &\leq \nu \left\| \mathbf{G}_k^t - \mathbf{H}_k(\mathbf{x}_k^{t+1}) \right\|^2 \\ &\leq \nu(1 + \epsilon) \left\| \mathbf{G}_k^t - \mathbf{H}_k(\mathbf{x}_k^t) \right\|^2 \\ &\quad + \nu(1 + \epsilon^{-1}) \left\| \mathbf{H}_k(\mathbf{x}_k^{t+1}) - \mathbf{H}_k(\mathbf{x}_k^t) \right\|^2,\end{aligned}$$

where, recall, $\nu = (1 - \alpha) \in [0, 1)$. Further, from the bounded gradient assumption—in particular, from (11)—we arrive at

$$\begin{aligned}\mathbb{E}_{\mathcal{F}'_t} \left[D_k^{(t+1)} \right] &\leq \nu(1 + \epsilon) D_k^{(t)} + \nu(1 + \epsilon^{-1}) H^2 \left\| \mathbf{x}_k^{t+1} - \mathbf{x}_k^t \right\|^2 \\ &= \nu(1 + \epsilon) D_k^{(t)} + \nu(1 + \epsilon^{-1}) \eta^2 H^2 \left\| \tilde{\mathbf{g}}_k^t \right\|^2,\end{aligned}$$

where, recall, $\tilde{\mathbf{g}}_k^t$ is our (possibly stochastic) update vector. Summing over $k = 0, 1, \dots, K$ and taking the nonconditional expectation of both sides of the inequality, we get that

$$\mathbb{E} D^{(t+1)} \leq \nu(1 + \epsilon) \mathbb{E} D^{(t)} + \nu(1 + \epsilon^{-1}) \eta^2 H^2 \mathbb{E} \left\| \tilde{\mathbf{g}}^t \right\|^2.$$

Lastly, using the fact that, under (A3), (A4) is equivalent to $\mathbb{E} \left\| \tilde{\mathbf{g}}^t \right\|^2 \leq \mathbb{E} \left\| \mathbf{g}^t \right\|^2 + \frac{\sigma_B^2}{B}$, we arrive at (7).

C Main Theorems

First, let us define some shorthand notation for terms we will be using throughout our proof, whose expectation is with respect to the (possible) randomness in the compression across all steps:

$$\begin{aligned}(\text{compression error}) \quad \Omega_1^t &:= \mathbb{E} D^{(t)}, \\ (\text{surrogate norm}) \quad \Omega_2^t &:= \mathbb{E} \left\| \mathbf{g}^t \right\|^2.\end{aligned}$$

C.1 Proof of Theorem 1

From the L -smoothness of f —more specifically, from (10)—we have that

$$\begin{aligned}f(\mathbf{x}^{t+1}) - f(\mathbf{x}^t) &\leq \langle \nabla f(\mathbf{x}^t), \mathbf{x}^{t+1} - \mathbf{x}^t \rangle + \frac{L}{2} \left\| \mathbf{x}^{t+1} - \mathbf{x}^t \right\|^2 \\ &= -\eta \langle \nabla f(\mathbf{x}^t), \tilde{\mathbf{g}}^t \rangle + \frac{\eta^2 L}{2} \left\| \tilde{\mathbf{g}}^t \right\|^2.\end{aligned}$$

Taking the conditional expectation over the batch selection, it follows from the unbiasedness of $\tilde{\mathbf{g}}^t$ (A3) that

$$\mathbb{E}_{\mathcal{F}_t} f(\mathbf{x}^{t+1}) - f(\mathbf{x}^t) \leq -\eta \langle \nabla f(\mathbf{x}^t), \mathbf{g}^t \rangle + \frac{\eta^2 L}{2} \mathbb{E}_{\mathcal{F}_t} \left\| \tilde{\mathbf{g}}^t \right\|^2.$$

From (A4), we have that $\mathbb{E}_{\mathcal{F}_t} \left\| \tilde{\mathbf{g}}^t - \mathbf{g}^t \right\|^2 \leq \frac{\sigma_B^2}{B}$, which, under (A3), is equivalent to $\mathbb{E}_{\mathcal{F}_t} \left\| \tilde{\mathbf{g}}^t \right\|^2 \leq \left\| \mathbf{g}^t \right\|^2 + \frac{\sigma_B^2}{B}$, so

$$\begin{aligned}\mathbb{E}_{\mathcal{F}_t} f(\mathbf{x}^{t+1}) - f(\mathbf{x}^t) &\leq -\eta \langle \nabla f(\mathbf{x}^t), \mathbf{g}^t \rangle + \frac{\eta^2 L}{2} \left\| \mathbf{g}^t \right\|^2 + \frac{\eta^2 L \sigma_B^2}{2B}\end{aligned}$$

$$\begin{aligned}
&= -\frac{\eta}{2}\|\nabla f(\mathbf{x}^t)\|^2 - \frac{\eta}{2}(1-\eta L)\|\mathbf{g}^t\|^2 \\
&\quad + \frac{\eta}{2}\|\mathbf{g}^t - \nabla f(\mathbf{x}^t)\|^2 + \frac{\eta^2 L\sigma^2}{2B},
\end{aligned}$$

where the last equation follows from the polarization identity $\langle a, b \rangle = \frac{1}{2}(\|a\|^2 + \|b\|^2 - \|a-b\|^2)$. Now, using our surrogate offset bound (6) and taking the (non-conditional) expectation, we get that:

$$\begin{aligned}
\mathbb{E}f(\mathbf{x}^{t+1}) - \mathbb{E}f(\mathbf{x}^t) &\leq -\frac{\eta}{2}\mathbb{E}\|\nabla f(\mathbf{x}^t)\|^2 - \frac{\eta}{2}(1-\eta L)\mathbb{E}\|\mathbf{g}^t\|^2 \\
&\quad + \frac{\eta KH^2 L^2}{2}\mathbb{E}D^{(t)} + \frac{\eta^2 L\sigma^2}{2B}.
\end{aligned} \tag{13}$$

Using the Ω_1^t and Ω_2^t notation defined earlier and recalling that $\nu = (1-\alpha) \in [0, 1)$, we rewrite (7) and (13), respectively, as

$$\Omega_1^{t+1} \leq \nu(1+\epsilon)\Omega_1^t + \nu(1+\epsilon^{-1})\eta^2 H^2 \Omega_2^t + \frac{\nu(1+\epsilon^{-1})\eta^2 H^2 \sigma^2}{B}$$

and

$$\begin{aligned}
\mathbb{E}f(\mathbf{x}^{t+1}) - \mathbb{E}f(\mathbf{x}^t) &\leq -\frac{\eta}{2}\mathbb{E}\|\nabla f(\mathbf{x}^t)\|^2 + \frac{\eta KH^2 L^2}{2}\Omega_1^t \\
&\quad - \frac{\eta}{2}(1-\eta L)\Omega_2^t + \frac{\eta^2 L\sigma^2}{2B}.
\end{aligned}$$

Multiplying the first inequality by a positive constant w and adding it to the second one, we get

$$\begin{aligned}
\mathbb{E}f(\mathbf{x}^{t+1}) - \mathbb{E}f(\mathbf{x}^t) + w\Omega_1^{t+1} - \psi_1(w)\Omega_1^t \\
\leq -\frac{\eta}{2}\mathbb{E}\|\nabla f(\mathbf{x}^t)\|^2 + \psi_2(w)\Omega_2^t \\
+ \left(w\nu(1+\epsilon^{-1})H^2 + \frac{L}{2} \right) \frac{\eta^2 \sigma^2}{B},
\end{aligned} \tag{14}$$

where

$$\psi_1(w) := w\nu(1+\epsilon) + \frac{\eta KH^2 L^2}{2}$$

and

$$\psi_2(w) := w\nu(1+\epsilon^{-1})\eta^2 H^2 - \frac{\eta}{2}(1-\eta L).$$

Looking at (14), we see that, if $\psi_2(w) \leq 0$, we can drop the Ω_2^t term. Further, if $\psi_1(w) \leq w$, we can telescope the Ω_1^t term as we sum the inequalities for $t = 0, \dots, T-1$, as we do for the $\mathbb{E}f(\mathbf{x}^t)$ terms. We thus get that:

$$\begin{aligned}
\frac{1}{T} \sum_{t=0}^{T-1} \mathbb{E}\|\nabla f(\mathbf{x}^t)\|^2 &\leq \frac{2(f(\mathbf{x}^0) - \mathbb{E}f(\mathbf{x}^T))}{\eta T} \\
&\quad + \frac{2w(\Omega_1^0 - \Omega_1^T)}{\eta T} \\
&\quad + (2w\nu(1+\epsilon^{-1})H^2 + L) \frac{\eta\sigma^2}{B},
\end{aligned} \tag{15}$$

for

$$w \in \mathcal{W}_\epsilon := \left\{ w : \frac{\eta KH^2 L^2}{2(1-\nu(1+\epsilon))} \leq w \leq \frac{1-\eta L}{2\eta H^2 \nu(1+\epsilon^{-1})} \right\},$$

where the lower bound follows from $\psi_1(w) \leq w$ and the upper bound from $\psi_2(w) \leq 0$.

Bounding η and choosing ϵ . To ensure that \mathcal{W}_ϵ is not empty, we need

$$\eta^2 \gamma(\epsilon) L^2 + \eta L \leq 1 \quad \text{where} \quad \gamma(\epsilon) := KH^4 \frac{\nu(1 + \epsilon^{-1})}{1 - \nu(1 + \epsilon)}.$$

From Lemma 5 of [Richtárik et al. \(2021\)](#), we know that, if $a, b > 0$, then $0 \leq \eta \leq \frac{1}{\sqrt{a+b}}$ implies $a\eta^2 + b\eta \leq 1$. Thus, we can ensure that \mathcal{W}_ϵ is not empty by requiring

$$\eta \leq \frac{1}{\sqrt{\gamma(\epsilon)L^2 + L}} = \left(\sqrt{\gamma(\epsilon)L} + L \right)^{-1}.$$

Further, to ensure that all $w \in \mathcal{W}_\epsilon$ are positive, we need $\nu(1 + \epsilon) < 1$, which holds for $\epsilon < \frac{1-\nu}{\nu}$. Thus, to have the largest upper bound possible on the stepsize η , we want ϵ to be the solution to the following optimization problem, solved in Lemma 3 of [Richtárik et al. \(2021\)](#):

$$\begin{aligned} \epsilon^* &:= \operatorname{argmin}_\epsilon \left\{ \tilde{\gamma}(\epsilon) := \frac{\nu(1 + \epsilon^{-1})}{1 - \nu(1 + \epsilon)} : 0 < \epsilon < \frac{1 - \nu}{\nu} \right\} \\ &= \frac{1}{\sqrt{\nu}} - 1. \end{aligned}$$

It follows that $\sqrt{\tilde{\gamma}(\epsilon^*)} = \frac{1 + \sqrt{1 - \alpha}}{\alpha} - 1$ and thus $\gamma(\epsilon^*) = KH^4 \left(\frac{1 + \sqrt{1 - \alpha}}{\alpha} - 1 \right)^2 =: \rho_{\alpha 1}$. We therefore need

$$\eta \leq \left(\sqrt{\gamma(\epsilon^*)L} + L \right)^{-1} = \left(\sqrt{\rho_{\alpha 1}L} + L \right)^{-1}.$$

Note that, for $\alpha = 1$, we recover $\eta \leq 1/L$.

Choosing w . Now, since $f^* \leq f(\mathbf{x})$ for all \mathbf{x} and $\Omega_1^T \geq 0$, we have from (15) that, for all $w \in \mathcal{W}_\epsilon$:

$$\begin{aligned} \frac{1}{T} \sum_{t=0}^{T-1} \mathbb{E} \|\nabla f(\mathbf{x}^t)\|^2 &\leq \frac{2\Delta}{\eta T} + \frac{2w\Omega_1^0}{\eta T} \\ &\quad + (2w\nu(1 + \epsilon^{-1})H^2 + L) \frac{\eta\sigma^2}{B}, \end{aligned}$$

where $\Delta := f(\mathbf{x}^0) - f^*$. From the inequality above, we see that we want $w \in \mathcal{W}_\epsilon$ to be as small as possible. Therefore, we take w to be the lower bound in \mathcal{W}_ϵ . Since $1 - \nu(1 + \epsilon^*) = 1 - \sqrt{\nu}$, this corresponds to setting $w = \frac{\eta KH^2 L^2}{2(1 - \sqrt{\nu})}$. Recalling that $\Omega_1^t = \mathbb{E}D^{(t)}$ and $\nu = 1 - \alpha$, we thus arrive at (8):

$$\begin{aligned} \frac{1}{T} \sum_{t=0}^{T-1} \mathbb{E} \|\nabla f(\mathbf{x}^t)\|^2 &\leq \frac{2\Delta}{\eta T} + \frac{KH^2 L^2}{1 - \sqrt{1 - \alpha}} \cdot \frac{\mathbb{E}D^{(0)}}{T} \\ &\quad + (\eta L \rho_{\alpha 1} + 1) \frac{\eta L \sigma^2}{B}. \end{aligned}$$

C.2 Proof of Theorem 2

Recall that, using the Ω_1^t and Ω_2^t notation, we can rewrite (7) and (13), respectively, as

$$\Omega_1^{t+1} \leq \nu(1 + \epsilon)\Omega_1^t + \nu(1 + \epsilon^{-1})\eta^2 H^2 \Omega_2^t + \frac{\nu(1 + \epsilon^{-1})\eta^2 H^2 \sigma^2}{B}$$

and

$$\begin{aligned} \mathbb{E}f(\mathbf{x}^{t+1}) - \mathbb{E}f(\mathbf{x}^t) &\leq -\frac{\eta}{2} \mathbb{E} \|\nabla f(\mathbf{x}^t)\|^2 + \frac{\eta KH^2 L^2}{2} \Omega_1^t \\ &\quad - \frac{\eta}{2} (1 - \eta L) \Omega_2^t + \frac{\eta^2 L \sigma^2}{2B}. \end{aligned}$$

Now, from our earlier introduced Lyapunov function (9), $V_t = \mathbb{E}f(\mathbf{x}^t) - f^* + c\Omega_1^t$, we have that:

$$\begin{aligned}
V_{t+1} &= \mathbb{E}f(\mathbf{x}^{t+1}) - f^* + c\Omega_1^{t+1} \\
&\stackrel{(i)}{\leq} \mathbb{E}f(\mathbf{x}^t) - f^* - \frac{\eta}{2}\mathbb{E}\|\nabla f(\mathbf{x}^t)\|^2 \\
&\quad + \left(\frac{\eta KH^2 L^2}{2} + c\nu(1+\epsilon)\right)\Omega_1^t + \psi_2(c)\Omega_2^t \\
&\quad + (L + 2c\nu(1+\epsilon^{-1})H^2)\frac{\eta^2\sigma^2}{2B} \\
&\stackrel{(ii)}{\leq} (1-\eta\mu)(\mathbb{E}f(\mathbf{x}^t) - f^*) \\
&\quad + \left(\frac{\eta KH^2 L^2}{2} + c\nu(1+\epsilon)\right)\Omega_1^t \\
&\quad + \psi_2(c)\Omega_2^t + (L + 2c\nu(1+\epsilon^{-1})H^2)\frac{\eta^2\sigma^2}{2B} \\
&= (1-\eta\mu)V_t \\
&\quad + \underbrace{\left(\frac{\eta KH^2 L^2}{2} + c\nu(1+\epsilon) - c(1-\eta\mu)\right)}_{=: \psi_3(c)}\Omega_1^t \\
&\quad + \psi_2(c)\Omega_2^t + (L + 2c\nu(1+\epsilon^{-1})H^2)\frac{\eta^2\sigma^2}{2B},
\end{aligned}$$

where (i) follows from (7), (13), $c > 0$, and $\psi_2(w) = w\nu(1+\epsilon^{-1})\eta^2 H^2 - \frac{\eta}{2}(1-\eta L)$ and (ii) follows from the PL inequality (A5). Looking the inequality above, we see that, if there is a c such that $\psi_2(c), \psi_3(c) \leq 0$, then

$$V_{t+1} \leq (1-\eta\mu)V_t + (L + 2cH^2\nu(1+\epsilon^{-1}))\frac{\eta^2\sigma^2}{2B}. \quad (16)$$

Note that, similarly to what we had in the proof for Theorem 1, $\psi_2(c) \leq 0$ corresponds to an upper bound on c , while $\psi_3(c) \leq 0$ corresponds to a lower bound on c . We therefore want $c \in \mathcal{W}'_\epsilon$, where

$$\mathcal{W}'_\epsilon := \left\{ c: \frac{\eta KH^2 L^2}{2(1-\nu(1+\epsilon)-\eta\mu)} \leq c \leq \frac{1-\eta L}{2\eta\nu(1+\epsilon^{-1})H^2} \right\}.$$

Recurring (16), we get

$$\begin{aligned}
V_T &\leq (1-\eta\mu)^T V_0 + (L + 2cH^2\nu(1+\epsilon^{-1}))\frac{\eta^2\sigma^2}{2B} \sum_{t=0}^{T-1} (1-\eta\mu)^t \\
&\leq (1-\eta\mu)^T V_0 + (L + 2cH^2\nu(1+\epsilon^{-1}))\frac{\eta\sigma^2}{2B\mu},
\end{aligned}$$

where the second inequality follows from the sum of a geometric series, arriving at the result we set out to prove.

Choosing ϵ and bounding η so that \mathcal{W}'_ϵ is nonempty. Note that the lower bound defining \mathcal{W}'_ϵ is positive if $\eta < \frac{1-\nu(1+\epsilon)}{\mu}$, where $1-\nu(1+\epsilon) > 0$ as long as $\epsilon < \frac{1-\nu}{\nu}$. Further, \mathcal{W}'_ϵ is not empty, as long as

$$\frac{\eta KH^2 L^2}{2(1-\nu(1+\epsilon)-\eta\mu)} \leq \frac{1-\eta L}{2\eta\nu(1+\epsilon^{-1})H^2},$$

which is equivalent to

$$\eta^2 L^2 (\beta_\epsilon(\alpha)KH^4 - \mu/L) + \eta L(\theta_\epsilon(\alpha) + \mu/L) \leq \theta_\epsilon(\alpha),$$

where

$$\theta_\epsilon(\alpha) = 1 - (1 - \alpha)(1 + \epsilon) \quad \text{and} \quad \beta_\epsilon(\alpha) = (1 - \alpha)(1 + \epsilon^{-1}).$$

If $\epsilon \leq \min\left\{\frac{1-\alpha}{\alpha}, \frac{\alpha}{1-\alpha}\right\}$, we have that $\beta_\epsilon(\alpha) \geq 1$ and $\theta_\epsilon(\alpha) \geq 0$ for all α . It follows from $\beta_\epsilon(\alpha) \geq 1$ that $\beta_\epsilon(\alpha) \geq 1KH^4 \geq KH^4 \geq H^4 \geq 1$, where the last inequality follows from (A2) holding for \mathbf{H}_0 . We thus get that

$$\eta^2 L^2 (1 - \mu/L) + \eta L(\mu/L) \leq \theta_\epsilon(\alpha). \quad (17)$$

Choosing ϵ to be

$$\epsilon^\star = \begin{cases} \alpha, & 0 < \alpha \leq 1/2, \\ 1 - \alpha, & 1/2 < \alpha \leq 1, \end{cases}$$

we get that

$$\theta_{\epsilon^\star}(\alpha) = \begin{cases} \alpha^2, & 0 < \alpha \leq 1/2, \\ -1 + 3\alpha - \alpha^2, & 1/2 < \alpha \leq 1. \end{cases}$$

Since $\alpha^2 \leq -1 + 3\alpha - \alpha^2$ for $\alpha \in (1/2, 1]$, we have that $\alpha^2 \leq \theta_{\epsilon^\star}(\alpha)$ for all $\alpha \in (0, 1]$. Thus, (17) holds if

$$\eta^2 L^2 (1 - \mu/L) + \eta L(\mu/L) \leq \alpha^2. \quad (18)$$

Further, from (A1) and (A5), we get that $0 \leq \mu/L \leq 1$. Therefore, for a sufficiently small η , there exists a positive $c \in \mathcal{W}'_\epsilon$ such that $\psi_2(c), \psi_3(c) \leq 0$. Lastly, note that we can also guarantee that $\eta < \frac{1-\nu(1+\epsilon^\star)}{\mu} = \theta_{\epsilon^\star}(\alpha)/\mu$ by having $\eta < \alpha^2/\mu$, which follows from (18).

Choosing c to minimize the upper bound. From (17), we see that we want c to be as small as possible. So, we choose c as the lower bound in the definition of \mathcal{W}'_ϵ , arriving at

$$V_T \leq (1 - \eta\mu)^T V_0 + \left(L + 2 \left(\frac{\eta K H^2 L^2}{2(1 - \nu(1 + \epsilon) - \eta\mu)} \right) H^2 \nu (1 + \epsilon^{-1}) \right) \frac{\eta \sigma^2}{2B\mu}.$$

Now, we know that, for $\epsilon = \epsilon^\star$ and $\eta^2 L^2 (1 - \mu/L) + \eta\mu \leq \alpha^2$, the lower bound in the definition of \mathcal{W}'_ϵ is less than or equal to the upper bound. We therefore have that

$$2 \left(\frac{\eta K H^2 L^2}{2(1 - \nu(1 + \epsilon) - \eta\mu)} \right) H^2 \nu (1 + \epsilon^{-1}) \leq \frac{1 - \eta L}{\eta}.$$

Using this inequality in the bound above it follows that

$$V_T \leq (1 - \eta\mu)^T V_0 + \frac{\sigma^2}{2B\mu},$$

thus arriving at the statement that we set out to prove.

D Comparison of different downlink communication schemes

As in most communication-compressed optimization literature (Haddadpour et al., 2021), our primary concern is uplink communications, which is typically the main bottleneck in training. Nevertheless, this appendix discusses three alternative downlink communication schemes in EF-VFL: **1**) the one in Algorithm 1, **2**) the one in Algorithm 2, and **3**) a modified version of the one in Algorithm 1 for common VFL fusion models, enabling broadcasts of a size that is independent of the number of clients, K . Approaches **1**) and **3**) are mathematically equivalent, yet Approach **2**) is not, as discussed earlier. Each approach has its pros and cons, making it suitable for different applications. For simplicity, this discussion focuses on top- k sparsification and the full-batch case.

1) In Algorithm 1, each round of downlink communications consists of a broadcast of size $k(K + 1)$ —a compressed object of size k for each client (the intermediate representations) and one for the server (the fusion model).

2) In Algorithm 2, each client receives only the derivative of the loss function with respect to its representation, resulting in a total downlink communication cost of kK . Recall that this is only an option when performing a single local update.

Approach **2)** avoids the dependency of the downlink communications to each client on K , seen in Approach **1)**, but requires K different communications (one to each client), rather than a single broadcast, thus the total communication cost still depends on K . The one-to-many nature of broadcasting makes it is more appropriate to compare broadcasted information with the total downlink communications, rather than the communication to a single client, as the latter ignores the cost of contacting the other $K - 1$ clients.

3) To ensure that the downlink communication cost does not depend on K , we can often exploit the structure of the fusion model ϕ . In particular, a common choice is $\phi(\mathbf{x}) = \phi_2(\mathbf{x}_0, \phi_1(\mathbf{H}_1(\mathbf{x}_1), \dots, \mathbf{H}_K(\mathbf{x}_K)))$, where ϕ_1 is a nonparameterized representation aggregator, such as a sum or an average, and ϕ_2 is a map parameterized by \mathbf{x}_0 . In this case, instead of broadcasting $K + 1$ objects, as in Approach **1)**, the server can broadcast the aggregation of the representations, $\phi_1(\{\mathbf{H}_j(\mathbf{x}_j^t)\})$. This allows us to collapse the dimension of length K , as long as each client i can replace $\mathbf{H}_i(\mathbf{x}_i^t)$ with $\mathbf{H}_i(\mathbf{x}_i^{t+1})$ in $\phi_1(\{\mathbf{H}_j(\mathbf{x}_j^t)\})$ using its local knowledge of its own representation. For example, if ϕ_1 is a sum, client i can subtract its previous intermediate representation and add the updated one to obtain an updated aggregation. This allows client i to perform forward and backward passes over both its local model and the fusion model, and thus perform multiple local updates without requiring further communications. Yet, this downlink communication of the aggregated representations will no longer be in the range of the compressor. For example, if \mathbf{v}_1 and \mathbf{v}_2 are within the range of top- k , their sum, $\mathbf{v}_1 + \mathbf{v}_2$, will generally not be. Therefore, we have a broadcast of up to size $N\bar{E} + d_0$, where d_0 is the size of the parameters of the fusion model. That is, we avoid the dependency on K , but this comes at the cost of losing the compressed nature of the downlink communications. (This sum may still lie in a lower-dimensional manifold, but this typically recovers the dependency on K , e.g., for top- k sparsification, we can upper bound the number of nonzero entries of the sum of K k -sparse vectors by $\min\{kK, N\bar{E}\} + d_0$.) Like Approach **1)**, Approach **3)** does not allow for private labels.

We present Approach **1)** in Algorithm 1, rather than Approach **3)**, because most VFL applications are in the cross-silo setting (Liu et al., 2024) and thus the number of clients K is small, therefore $k(K + 1) \ll N\bar{E} + d_0$. Yet, for applications where K is large, Approach **3)** may be preferable.